Food and Chemical Toxicology 152 (2021) 112164

Contents lists available at ScienceDirect

Food and Chemical Toxicology

journal homepage: www.elsevier.com/locate/foodchemtox

Oral subchronic exposure to the mycotoxin ochratoxin A induces key pathological features of Parkinson's disease in mice six months after the end of the treatment

María Izco [a], Ariane Vettorazzi [b,c,*], Raquel Forcen [a], Javier Blesa [d], Maria de Toro [e], Natalia Alvarez-Herrera [a], J Mark Cooper [f], Elena Gonzalez-Peñas [g], Adela Lopez de Cerain [b,c], Lydia Alvarez-Erviti [a,**]

[a] Laboratory of Molecular Neurobiology, Center for Biomedical Research of La Rioja (CIBIR), Piqueras 98, 3rd Floor, 26006, Logroño, Spain
[b] Department of Pharmacology and Toxicology, MITOX Research Group, Universidad de Navarra, Pamplona, 31008, Spain
[c] IdiSNA, Navarra Institute for Health Research, Pamplona, 31008, Spain
[d] HM CINAC, Hospital Universitario HM Puerta del Sur, Av. Carlos V, 70, 28938, Móstoles, Madrid, Spain
[e] Genomics and Bioinformatics Core Facility, Center for Biomedical Research of La Rioja (CIBIR), Logroño, Spain
[f] Department of Clinical and Movement Neuroscience, Institute of Neurology, UCL, Gower Street, London, UK
[g] Department of Pharmaceutical Technology and Chemistry, Universidad de Navarra, Pamplona, 31008, Spain

ARTICLE INFO

Handling Editor: Dr. Jose Luis Domingo

Keywords:
Parkinson's disease
Alpha-synuclein
Ochratoxin A
Gut-brain axis
Chaperone-mediated autophagy
LAMP-2A

ABSTRACT

Some epidemiological studies with different levels of evidence have pointed to a higher risk of Parkinson's disease (PD) after exposure to environmental toxicants. A practically unexplored potential etiological factor is a group of naturally-occurring fungal secondary metabolites called mycotoxins. The mycotoxin ochratoxin A (OTA) has been reported to be neurotoxic in mice. To further identify if OTA exposure could have a role in PD pathology, Balb/c mice were orally treated with OTA (0.21, 0.5 mg/kg bw) four weeks and left for six months under normal diet. Effects of OTA on the onset, progression of alpha-synuclein pathology and development of motor deficits were evaluated. Immunohistochemical and biochemical analyses showed that oral subchronic OTA treatment induced loss of striatal dopaminergic innervation and dopaminergic cell dysfunction responsible for motor impairments. Phosphorylated alpha-synuclein levels were increased in gut and brain. LAMP-2A protein was decreased in tissues showing alpha-synuclein pathology. Cell cultures exposed to OTA exhibited decreased LAMP-2A protein, impairment of chaperone-mediated autophagy and decreased alpha-synuclein turnover which was linked to miRNAs deregulation, all reminiscent of PD. These results support the hypothesis that oral exposure to low OTA doses in mice can lead to biochemical and pathological changes reported in PD.

1. Introduction

Parkinson's disease (PD) is a neurodegenerative disorder pathologically characterized by the loss of dopaminergic (DA) neurons in the substantia nigra pars compacta (SNc) and the presence of Lewy bodies (LB) aggregates, which contain phosphorylated alpha-synuclein (Fearnley et al., 1991; Simón-Sánchez et al., 2009). While LB are predominantly found within the brain, they are also found in the periphery including the peripheral nervous system (Comi et al., 2014). The factors initiating or contributing to the pathogenesis of PD are still largely unclear for the majority of patients; however, recent findings of genetic causes and environmental risk factors are beginning to highlight important pathogenic pathways (Johnson et al., 2018a). The preclinical stage of PD is associated with impairment in olfaction and gastrointestinal dysfunction, two non-motor symptoms that can manifest even decades before the onset of the motor abnormalities (Schapira et al., 2017). Affecting up to 80% of PD patients, constipation represents the most frequent gastrointestinal dysfunction in PD (Cersosimo et al.,

* Corresponding author.
** Corresponding author.
E-mail addresses: mizco@riojasalud.es (M. Izco), avettora@unav.es (A. Vettorazzi), r.forcen.90@gmail.com (R. Forcen), jblesa.hmcinac@hmhospitales.com (J. Blesa), mthernando@riojasalud.es (M. de Toro), nalvarezhe@gmail.com (N. Alvarez-Herrera), jmark.cooper@ucl.ac.uk (J.M. Cooper), mgpenas@unav.es (E. Gonzalez-Peñas), acerain@unav.es (A. Lopez de Cerain), laerviti@riojasalud.es (L. Alvarez-Erviti).

https://doi.org/10.1016/j.fct.2021.112164
Received 22 January 2021; Received in revised form 25 March 2021; Accepted 29 March 2021
Available online 2 April 2021

2013) and patients with a previous diagnosis of constipation have an increased risk of developing PD (Stirpe et al., 2016). This early non-motor symptom affects the gut, an organ exposed to the environment, and could link to exposure of factors that initiate PD pathogenesis. This hypothesis is reinforced by data suggesting that LB pathology can be found in the large intestine in PD patients up to 20 years before the diagnosis of PD (Stockholm et al., 2016). The link to LB pathology in the brain has been suggested to involve the spread of pathological alpha-synuclein from the enteric nervous system (ENS), via axonal transport through the vagal nerve, to the lower brainstem, a process that precedes DA neurons degeneration (Braak et al., 2003). This caudal-rostro, prion-like, cell-to-cell progression of alpha-synuclein pathology is also known as Braak's hypothesis (Braak et al., 2003; Hawkes et al., 2007) and has also been supported in experimental models (Kim et al., 2019; Anselmi et al., 2018). This mechanism in PD has been recently supported by a study showing a decreased risk of PD in patients who underwent truncal vagotomy (Svensson et al., 2015).

Although olfactory and gastrointestinal symptoms have been documented in pesticide-based animal models of PD (Sasajima et al., 2015; Johnson et al., 2018b), human empirical evidence is sparse and indirect. One study in North Carolina found that non-farming laborers were able to detect odors at significantly lower concentrations than farmworkers (Quandt et al., 2016), however the study could not directly attribute this observation to pesticide use or toxin exposure. Some epidemiological studies with different levels of evidence have pointed to a higher risk of PD after exposure to environmental toxicants (for extensive reviews, check Goldman, 2014; Marras et al., 2019). Indeed, people living in rural areas have been described to have a significantly increased risk of suffering PD, which may be related to exposure to potential neurotoxins present in crops, pesticides, well water or spring water (Gorell et al., 1998; Priyadarshi et al., 2001). The most consistent epidemiological evidence comes from studies that specifically focused on pesticides (Van der Mark et al., 2012) although the specific pesticides or classes responsible for this association have yet to be identified (Hatcher et al., 2008).

Some of these environmental toxicants have also partially reproduced the characteristics of PD in animal models. Indeed some of them are widely used for animal models for PD, such as rotenone (Betarbet et al., 2000), 1-methyl-4-phenyl-1,2,3,6-tetrahydropyridine (MPTP) (Langston and Ballard, 1983), paraquat (Brooks et al., 1999) and maneb (Zhang et al., 2003). All these toxins produce oxidative stress, neuroinflammation and dopaminergic cell death but do not mimic other key features of PD including the development of alpha-synuclein aggregates throughout the brain and the progression of the pathology. Therefore, the experimental evidence that these toxins can trigger PD in humans still remains unclear.

Another highly relevant group of naturally-occurring agricultural toxins, present in the environment long before pesticides, are mycotoxins to which humans are widely exposed mainly through diet (BIOMIN, 2018) but also by inhalation (Niculita-Hirzel et al., 2016; Viegas et al., 2018). Indeed, in the last report of the European Rapid Alert System for Food and Feed (RASFF), "mycotoxins" (aflatoxins and ochratoxin A) was among the top 10 most frequently hazard notified at EU level and was the most reported type of hazard for food products from non EU countries (RASFF, 2019). They are known to induce important adverse health effects in humans (Marin et al., 2013; Janik et al., 2020), including long-term diseases such as cancer (Vettorazzi et al., 2016). Nowadays the toxicological evaluation of cocktails of mycotoxins is a big challenge in the field of food safety evaluation (Dellafiora and Dall'Asta, 2017). It has been recently estimated that the worldwide prevalence of mycotoxins is up to 60–80% (Eskola et al., 2019). However, although the literature about mycotoxins is rich in reports investigating cellular mechanisms, cellular toxicity, associated pathology and animal toxicity (for recent reviews check Adaku Chilaka et al., 2020; Marin et al., 2013; Janik et al., 2020), these toxins have been practically unexplored as etiological agents of neurodegenerative diseases. One of the most important mycotoxins in terms of toxicity and exposure is ochratoxin A (OTA). Indeed, OTA is one of the most prevalent mycotoxins worldwide (BIOMIN, 2018) and human exposure is continuous (Arce-López et al., 2020) although at low levels. Due to its nephrotoxicity and potential carcinogenicity (EFSA, 2006; EFSA 2020) maximum limits (from 0.5 to 80 μg/kg) have been laid down for certain food commodities (EC, 2006).

This mycotoxin is a potent renal carcinogen in rodents (Lock and Hard, 2004) and has been classified as "probably carcinogenic to humans" (Group 2A) by the International Agency for Research on Cancer (IARC, 1993) as well as "reasonably anticipated to be a human carcinogen" by the National Toxicology Program of the USA (NTP, 2016). Although the mode of action (MoA) of OTA toxicity and carcinogenicity remains unclear (EFSA, 2006; WHO World Health Organization, 2008), some mechanisms have been hypothesized to totally or partially explain its MoA as a carcinogen (WHO World Health Organization, 2008). Some of them like mitochondrial dysfunction, oxidative stress production and alterations of calcium homeostasis might also be relevant for neurodegenerative diseases. Indeed, 2 μM of OTA has been shown to exert neurotoxicity in human astrocytes through mitochondria-dependent apoptosis and intracellular calcium overload (Park et al., 2019). Regarding OTA specific neurotoxic effects, it has shown to increase the expression of genes involved in the brain inflammatory system and to reduce the expression of glial fribrillary acidic protein in brain cells in vitro in range of 10–20 nM (Zurich et al., 2005). OTA has also reduced cell viability, induced the transcription factor activator (AP-1) and nuclear factor kappa B (NF-κB) at 0.5 and 1 μg/mL and inhibited neurite outgrowth at higher concentrations in rat embryonic midbrain cells (Hong et al., 2002). *In vivo*, OTA induced behavioral alterations in zebrafish (Khezri et al., 2018), reached the brain after oral administration in rats (Belmadani et al., 1998a) and was also reported to be neurotoxic to adult male rats orally treated with OTA for 8 days (289 μg/kg bw) (Belmadani et al., 1998b). In respect to pathological features associated with PD, a single intraperitoneal administration of a high dose of OTA (3.5 mg/kg bw) caused striatal dopamine depletion and decreased tyrosine hydroxylase (TH) immunoreactivity (Sava et al., 2006a). Moreover, the depletion in the striatal levels of dopamine was also observed after continuous subcutaneous administration of high doses of OTA (4–12 mg/kg bw) for two weeks (Sava et al., 2006b). The OTA induced dopaminergic striatal dysfunction was associated with motor abnormalities that were reversed by L-dopa administration (Bhat et al., 2018).

To gain insights into the role of OTA exposure on the features associated with PD, we studied the long-term effects of oral exposure to low doses of OTA on the changes in dopaminergic neurons, onset and progression of alpha-synuclein pathology and on the development of motor deficits in wild type (WT) Balb/c mice. Male mice were administered with OTA (0.21 or 0.5 mg/kg bw) by oral gavage daily for 28 days and left for 6 months under normal diet. The exposure conditions selected (0.21 or 0.5 mg/kg bw by gavage for 4 weeks) are considered as very low doses for mice, as the lowest observed effect level for kidney tumors was 4.4 mg/kg bw (administered in diet) in 2 years bioassay (EFSA, 2006). Our results showed that oral subchronic treatment with low-doses of OTA induced alpha-synuclein accumulation in the gut and thereby induces PD-like pathological progression to central nervous system (CNS). We also demonstrated that OTA exposure causes significant motor deficits 6 months after the end of the treatment, associated with a loss of DA innervation and DA neuron dysfunction in the SNc. Using cell models we confirmed that OTA exposure caused a decrease in LAMP-2A protein associated with the dysregulation of miRNAs, this in turn leads to decreased chaperone-mediated autophagy (CMA) activity and increased alpha-synuclein levels. The influence of pathological changes in alpha-synuclein upon LAMP-2A protein was confirmed in the alpha-synuclein preformed fibrils (PFF) mouse model. All these factors have been previously described in PD indicating that short term oral exposure to low doses of OTA can replicate the mechanistic features

observed in PD.

2. Material and methods

2.1. Animals

Eight-to nine-week-old male Balb/c mice (n = 70) for OTA studies and C57BL6/C3H F1 mice (n = 24) of the same age and sex for the PFF model were purchased from Charles River. All animals were randomly distributed to the cages and before any procedure, the cages were randomized to each group by a person not involved in the study. Animals were housed in individual polycarbonate cages with stainless steel covers, with a maximum of five mice per cage. All mice were allowed to ad libitum access to standard pellet diet (Special Diet Service, UK) and normal tap water and were maintained in constant environmental conditions of humidity (55 ± 10%) and temperature (22 ± 2 °C) on a 12-h light/dark cycle. All the in vivo experiments were blinded and the investigators responsible for data collection and analysis were blinded. These studies was approved by the Ethics Committee on Animal Experimentation of the Center of Biomedical Research of La Rioja (CIBIR, permit number LAE-02, LAE-04) and was conducted according to the National Institute of Health (NIH) Guide for the Care and Use of Laboratory.

2.2. OTA

OTA was purchased in powder from Sigma and was dissolved in 0.10 M $NaHCO_3$ (pH 7.4) for animal and cell culture treatments, and in methanol 99.9% (Panreac) in order to prepare the stock solutions needed for chromatographic analysis. Then, OTA-solutions were aliquoted and maintained at −20 °C until use.

2.3. Study design

Two different mouse strains were used in this research, Balb/c mice and C57BL6/C3H F1 mice. Balb/c is a mouse strain widely used for general experimental studies in toxicology and is the strain used in immunotoxicological OTA studies (Thuvander et al., 1995) and has been shown to be a suitable strain for long term toxicity studies with OTA (Stoev, 2020). Moreover, this strain was also selected based on the fact that it is less sensitive to more immediate neurotoxic effects caused by DA toxicants as MPTP (Ito et al., 2013). C57BL6/C3H F1 is a hybrid mouse strain used for the alpha-synuclein PFF model (Luck et al., 2012).

First, a preliminary study was carried out to select OTA doses. Balb/c mice received repeated OTA administrations (0.21, 0.5, 1.5 and 4.5 mg/kg bw) or vehicle ($NaHCO_3$) daily for 28 days by oral gavage (n = 9, except the group treated with OTA 4.5 mg/kg n = 4). The volume of the administration was 5 mL/kg, therefore the animals were weighed daily in order to adjust the volume and the dose administrated to the animal weight. Mice were sacrificed by overdose of inhaled isofluorane 1 day after the end of the OTA treatment and blood was collected by cardiac puncture at sacrifice. The brains were rapidly removed and sectioned longitudinally. The right hemispheres were dissected, immediately frozen on liquid nitrogen and stored at −80 °C until its use for biochemical analysis, while the left hemispheres were fixed in 4% paraformaldehyde at 4 °C, cryoprotected in 30% sucrose, frozen and stored at −80 °C until its use for immunohistochemical analysis.

For the long-term effect OTA study, Balb/c mice were randomly distributed into 3 groups of 10 mice per group. After one week of acclimatization, the animals received repeated OTA administrations (0.21 or 0.5 mg/kg) or vehicle ($NaHCO_3$) daily for 28 days by oral gavage. The volume of the administration was 5 mL/kg, therefore the animals were weighed daily in order to adjust the volume and the dose administrated to the animal weight. Mice were sacrificed by overdose of inhaled isofluorane 27 weeks after the end of the OTA treatment, blood was collected by cardiac puncture and the brains and distal intestines were rapidly removed. The brains were sectioned longitudinally and right and left hemispheres processed as described in the preliminary study. Distal intestines were divided in two pieces, one piece was immediately frozen for biochemical analysis and the other one was fixed, cryoprotected and frozen for histological analysis.

For the PFF model, C57BL6/C3H F1 mice (n = 6 per group and timepoint) were deeply anesthetized with isoflurane and received two 2.5-μl injections of sonicated murine alpha-synuclein PFF (5 μg) or PBS into the dorsal right striatum (5 μl total; coordinates: AP +0.2, ML -2.0, DV -3.4 and −2.6 from the skull) as previously described (Luck et al., 2012). Injections were performed using a 10 μL syringe (Hamilton) at a rate of 0.25 μL per min with the needle in place at each site of injection for 5 min after injection to prevent backflow. Control animals were injected with an equal volume of sterile PBS. Mice were sacrificed at various time points 15, 30 and 90 days post injection (dpi) by overdose with isoflurane, brains were dissected into different brain regions and immediately frozen and stored at −80 °C until used for biochemical analyses.

For the in vitro assays, an established human SH-SY5Y neuroblastoma cell line clone over-expressing full-length WT human alpha-synuclein with a C-terminal haemagglutinin (HA) tag was culture in 1:1 mixture of Dulbecco's modified Eagle's medium and Ham's F12 medium supplemented with 10% fetal bovine serum, 0.01 μM nonessential amino acid and penicillin/streptomycin (Alvarez-Erviti et al., 2013). A Caco-2 cell line (a cell line derived from a human colorectal adenocarcinoma used in the models of the intestinal epithelium (Costa and Ahluwalia, 2019)) was culture in of Dulbecco's modified Eagle's medium supplemented with 10% fetal bovine serum and penicillin/streptomycin and was transiently tranfected with a plasmid to over-express full-length WT human alpha-synuclein with a C-terminal HA tag. Both cell lines were treated for 72 h with OTA (50, 100 and 200 nM), which is the optimal timepoint to detect alpha-synuclein accumulation in these cell models.

2.4. Clinical examinations and body weights

All animals were observed weekly for detecting any gross abnormalities or changes in clinical conditions, like poorly groomed fur, bald patches in the coat or absence of whiskers, labored breathing or other easily observable symptoms which can lead to unusual home cage behaviour, with standard arena observations. Additionally, the body weight was recorded daily during OTA treatment and weekly thereafter until sacrifice. Postmortem examination was carried out to detect macroscopic changes of tissues and organs.

2.5. Behavioral assessments

To evaluate the motor function, mice were tested on wire hang and negative geotaxis tests before treatment, at 30 day intervals during the study and prior to sacrifice. Both tests were performed on the same animals. All tests were conducted between 09:00–13:00 in the lights-on cycle to eliminate time of day differences in behaviour and mice were allowed to rest in 30 min between tests. Mice were habituated to testing room 1 h before tests and the apparatus were cleaned with 70% ethanol in between animals to minimize odor cues.

2.5.1. Wire hang test

To assess neuromuscular strength and motor coordination, the wire hang test was performed. Each mouse was placed on a wire lid of a conventional housing cage. The lid was lightly agitated to encourage the animals gripping of the bars and then was turned upside down. The latency of mice to fall off the wire grid was measured and averaged over two trials (15 min apart). Trials were stopped if the mouse remained on the lid for over 15 min.

2.5.2. Negative geotaxis

Motor coordination was assessed in an inclined plane. Each mouse was placed with its head facing downward on a wire grid that was set at a 45° angle to the plane. The behaviour of the animal was observed during 30 s and scored as follows: 0 = turns and climbs, 1 = turns and freezes, 2 = moves, but fails to turn, 3 = does not move (Susick et al., 2014). The latency to turn 180° to an upright position and initiate climbing was recorded for all animals that received a score of 0. If the mouse was unable to turn, the default value of 30 s was taken as maximal severity of impairment.

2.6. Plasma collection

Blood collection was carried out at sacrifice when mice were deeply anesthetized with an overdose of inhaled isofluorane and bled by cardiac puncture. Blood samples (1 mL) were collected into EDTA-coated vials (Multivette® 600 K3E, Sarstedt) and were centrifuged at 2000×*g* for 10 min at 4 °C to obtain plasma fraction, which were stored at −80 °C until its use for OTA determination.

2.7. Chromatographic determination of OTA in brain and plasma samples

For OTA quantification, a previously validated method for this toxin analysis in rat biological samples (Vettorazzi et al., 2008) was revalidated for mice tissues. Briefly, OTA was quantified by HPLC-FLD in an 1100 series LC (Agilent Technologies, Germany) with fluorescence detection (λ excitation 225 nm and λ emission 461 nm). The chromatographic system was equipped with a Tracer Extrasil ODS column (25 cm × 0.4 cm, 5 μm particle size) from Teknokroma (Spain) and working at 40 °C. The mobile phase, pumped at 1 mL/min, was a mixture of acetonitrile and an aqueous solution of formic acid (0.4%) (50:50) in isocratic conditions. Acetonitrile and formic acid were from Merck (Germany).

Brain samples were weighted and mixed with a sodium dihydrogen phosphate buffer solution at pH 6.5 by vortexing (4 μL per mg of brain). Then the mixture was sonicated during 30 min and frozen at −80 °C during 24 h. Extraction of OTA form the buffer solution or plasma was made using acetonitrile acidified with formic acid (0.4%). Calibrators were prepared in mobile phase and the ranges studied were 2–20 ng/mL and 20–200 ng/mL. Both calibration curves met the previously stablished performance criteria. Recovery was assessed by spiking brain or plasma blank samples with OTA at three concentration levels and in intermediate conditions. Recovery was evaluated as the relation between mean OTA peak area in brain or plasma samples and mean OTA peak area in calibrators for each concentration level. The obtained recovery values were 97.9% from plasma samples and 65.9% from brain samples. These values have been taken into account in the quantification. The limits of quantification (LOQ) were 0.02 ng/mg and 2 ng/mL in brain and plasma samples, respectively.

2.8. Immunohistochemistry

30-μm-thick coronal brain and 8-μm-thick transversal distal intestine sections were prepared using a cryostat. Slices were washed with PBS and were incubated with 3% hydrogen peroxidase in PBS to inactivate the endogenous peroxidase. The slices were washed in PBS and were incubated with a blocking solution (0.1 M PBS containing 5% NGS 0.04% Triton X-100) for 1 h. Slices were incubated 24 h at 4 °C with the primary antibodies: anti-TH (Abcam) or phospho S129 anti-alpha-synuclein (Abcam). Slices were washed with PBS and were then incubated with biotinylated secondary antibody polyclonal goat anti-rabbit biotinylated (Dako). All the samples were processed simultaneously to obtain similar staining intensity.

The total number of dopaminergic (TH-positive) neurons in the SNc was assessed by stereology with the optical fractionator method in regularly spaced 30 μm-thick sections (every forth) with a total of 8–12 sections per animal spanning the entire rostro-caudal axis of the SNc (Kett et al., 2015; Brichta et al., 2015). This method was carried out by using a computer-assisted image analysis system consisting of a microscope (Olympus BX3) equipped with a computer controlled motorized stage, a camera, and the StereoInvestigator software (Stereo Investigator; MicroBrightField, VT, USA). The identification of the SNc region to be counted on each section was outlined at 4 × magnification and immunolabelled cells were counted with a 100x oil immersion objective (counting frame, 50 × 50 μm; sampling grid, 125 × 100 μm). The first section was randomly selected. Cells exhibiting neuronal phenotype, with a clear nuclear membrane, distinct nucleolus, and TH-immunoreactivity in the cytoplasm, were counted through the entire thickness of the tissue by a researcher 'blinded' to the treatment regimen of each experimental animal assessed. After counting was finished, the total number of neurons was automatically calculated by the software using the formula described by West et al. (West, 1993). Animals with less than 8 consecutive sections containing TH positive neurons were excluded from the analysis.

Striatal optical density (OD) of TH immunostaining was used as an index of the density of striatal dopaminergic innervation. This was determined by image analysis using the Image J program (National Institutes of Health, USA). All samples were processed at the same time and digital images were captured under the same exposure settings for all experimental analyses. Briefly, six representative rostro-caudal sections (at three levels of the striatum) were examined for each animal and regions of interest in the striatum were delineated and pixel densities were estimated using ImageJ. Background staining was quantified by measurement of pixel intensities in the white matter and subtracted from striatal regions for normalization.

For assessment of pathologic alpha-synuclein aggregates in the SNc, 4 coronal sections throughout the rostrocaudal extent of the SNc (240 μm intervals between sections, 1/8 series) for each animal were labelled using antibody against S129 phospho-alpha-synuclein. The SNc region was defined with the 5x objective using both the Paxinos and Franklin Mouse Brain Atlas and the areas occupied by TH positive neurons in the serial TH-stained sections covering the entire extent of the SNc destined for stereological estimation of dopaminergic neurons. Numbers of S129 phospho-alpha-synuclein inclusions present in the defined SNc region were manually counted at 20x magnification. The data represent the total number of aggregates per section or SNc region. In intestine sections, estimation of the percentage of immunostained area occupied by S129 phospho-alpha-synuclein inclusions was carried out using ImageI software (NIH). In some analysis, fewer samples were analyzed as there was no enough sample.

2.9. Western blot

Frozen midbrain, brainstem and cerebral cortex samples (n = 10 per group of OTA treated mice and n = 6 per group from the PFF model. In some analysis, fewer samples were analyzed as there was no enough sample), distal intestine tissue (n = 5 per group) or cell samples (n = 4 independent experiments) were homogenized in a 10 mM Tris/HCl (pH 7.4) buffer containing 0.1% sodium dodecylsulfate, a protease inhibitor mixture (Halt protease inhibitor cocktail, Thermo Scientific), phosphatase inhibitor (Halt phosphatase inhibitor cocktail, Thermo Scientific) and DNAse (RQ1 DNase, Promega). Proteins levels were determined by the Pierce BCA protein assay (Pierce BCA protein assay kit, Thermo Scientific) using bovine serum albumin as the standard. Samples (20 μg of protein) were solubilised in LDS buffer (Invitrogen) and reducing agent (Invitrogen) and separated on NuPAGE Novex 4–12% Bis-Tris Gels (Invitrogen), transferred to PVDF membrane and analyzed by Western blot as previously described (Alvarez-Erviti et al., 2013) using the following primary antibodies: anti phospho S129 alpha-synuclein (Abcam), anti alpha-synuclein (Abcam), anti LAMP-2A (Abcam), anti hsc70 (Abcam) and anti beta-actin (Abcam) antibodies. Membranes were incubated with horseradish peroxidase-conjugated secondary

antibodies (Polyclonal goat anti mouse Ig HRP and Polyclonal goat anti rabbit Ig HRP, Dako) which were detected using ECL Western Blot Substrate (Pierce ECL Western blotting substrate, Thermo Scientific) and Hyperfilm ECL (GE Healthcare). The membranes were reproved for beta-actin. Films were scanned, alternatively LAMP-2A and hsc70 signals were detected using the ChemiDoc MP Imaging System (Bio-Rad). Signals in the linear range were quantified using Image J and normalized to beta-actin levels.

2.10. Study of alpha-synuclein half-life

Alpha-synuclein turnover was assessed using a standard cycloheximide procedure (25 μg/mL) (Alvarez-Erviti et al., 2010). SH-SY5Y cells were treated with cycloheximide to inhibit protein synthesis and the cell samples removed at 12-h intervals up to 48 h. Sample loadings from equal cell numbers were calculated using the fluorescent DAPI assay of DNA content. Alpha-synuclein was detected by Western blots and were analyzed using Image J. Half-life was calculated using linear regression model; average half-life was calculated from regression lines drawn for each individual experiments using Excel.

2.11. Quantitative PCR

Total RNA was isolated from cell samples (n = 4) and midbrain samples from PFF mice (n = 5) using the RNeasy Mini kit (Qiagen) as per manufacturer's protocol. Reverse transcription (RT) was performed with Precision nanoScript2 RT kit (Z-RT-nanoScript2, Primer Design) as per manufacturer's instruction. Transcripts obtained from the reverse transcriptase reaction were analyzed for *lamp-2a* and *hsc70* quantification by quantitative real-time PCR. qPCR experiments were performed on a StepOneTM Real-Time PCR system (Applied Biosystems) using NZYSpeedy qPCR master mix (NZYtech). Values were calculated using the standard ΔΔCt method relative to actin. The primer sequences for *lamp-2a* (forward: 5′-TATGTGCAACAAAGAGCAGA-3'; reverse: 5′-CAGCATGATGGTGCTTGAGA-3′) and *hsc70* (forward: 5′- ATTGATCTTGGCACCACCTA-3'; reverse: 5′- ACATAGCTTGAAGTGGTTCG-3′) (Alvarez-Ervit et al., 2013) were synthesized by Sigma and the sequence for mouse actin (forward: 5′- TCTACAATGAGCTGCGTGTG-3'; reverse: 5′- GGTGAGGATCTTCATGAGGT-3′) and human actin (forward: 5′-TCTACAATGAGCTGCGTGTG-3'; reverse: 5′-GGTGAGGATCTTCATGAGGT-3) was synthesized by Primer Design.

2.12. miRNA analysis

Total RNA was harvested from SH-SY5Y using the miRNeasy Mini kit for cell culture (Qiagen) as per the manufacturer's protocol. Sequencing libraries for smallRNA analysis were prepared using TruSeq smallRNA Library Prep kits (Illumina), the small-RNA samples were sequenced using the Illumina MiSeq platform. miARma-Seq tool (Andrés-León et al., 2016) was used to analyze the data. The analysis was carried out by removing adaptor and low quality sequences. The remaining sequences were filtered and the sequences between 19 bp to 25 bp were obtained. The filtered sequences were considered for annotation. Firstly, the sequences were mapped against the *Homo sapiens* Hg19 reference genome plus the miRBase version 21 database with Bowtie1 (http://ccb.jhu.edu/software/tophat/index.shtml). The expression of miRNAs in treated and control libraries was compared by using the edgeR package, integrated into miARma-Seq tool.

2.13. miRNA luciferase assay

For the miRNA luciferase analysis SH-SY5Y cells were transfected with 1 μg of luciferase-3′UTR *lamp-2a* plasmid (Alvarez-Erviti et al., 2013) and 1 μl of X-tremeGENE HP transfection reagent (Roche) as per the manufacturer's instructions in 24-well plates with 105 cells per well. At 4 h after transfection, cells were treated with 100 nM hsa-miR-193a-3p. Luciferase activity was measure after 48 h with Dual-Glo Luciferase Assay System (Promega) using a luminometer.

2.14. Statistical analysis

Homogeneity of variance was assessed using Levene's test. Statistical analyses of the data were performed using SPSS program (version 25.0) using the non-parametric Kruskall-Wallis and Mann-Whitney *U* test for in vitro assays and parametric one-way ANOVA followed by the Tukey HSD test for in vivo analysis. Behavioral test were analyzed by two way ANOVA repeated test analysis performed using GraphPad Prism 6. A probability level of 0.05 or less was considered to be statistically significant. *p < 0.05, **p < 0.01, ***p < 0.001.

3. Results

A preliminary study aimed to select OTA doses was performed, in this study Balb/c mice received a daily oral gavage of OTA (0.21, 0.5, 1.5 and 4.5 mg/kg bw) or vehicle every day for 4 weeks and were sacrificed the day after the last dose of OTA. No clinical signs of toxicity were observed during the study in the animals treated with 0.21, 0.5, 1.5 mg/kg OTA, but the body weight of the 1.5 mg/kg OTA group showed a lower increase (Supp Fig 1a). A clear toxicity associated with an important decrease in body weight was observed in the group treated with 4.5 mg/kg OTA (Supp Fig 1a) and one animal was sacrificed due to the toxicity.

OTA was detectable in plasma samples in all the treated groups (Supp table 1). The increase of OTA concentration in plasma was dose dependent (Supp Fig 1b). Brain OTA concentrations in mice treated with 0.21 and 0.5 mg/kg OTA were under the LOQ in most cases, and low concentrations of OTA were measured in the groups treated with 1.5 and 4.5 mg/kg OTA (Supp table 1). The effect of OTA treatment in the nigrostriatal DA pathway was assessed. There were no differences in the DA innervation in striatum (Supp Fig 1c) and in the number of TH+ DA neurons (Supp Fig. 1d and e) in SNc in OTA-treated mice compared to control mice.

On the basis of these results the two lower doses (0.21 and 0.5 mg/kg) were selected for the study to assess long-term effects.

3.1. Clinical examinations, body weights and OTA levels

To investigate if subchronic treatment with low doses of OTA induces PD-related pathology, Balb/c mice received a daily oral gavage of OTA (0.21 or 0.5 mg/kg bw) or vehicle every day for 4 weeks and were monitored for another 6 months. One control was excluded from the study due to a pathological abnormality in the brain unrelated with the treatment, this finding is present in a low percentage of WT mice. No clinical signs of toxicity were observed during the study and OTA treatment did not affect body weight (Supp Fig 2). OTA was undetectable (<LOQ) in plasma and brain tissue samples 6 months after the last administration (data not shown).

3.2. Effect of subchronic oral OTA treatment in motor function

Motor performance was evaluated every week during OTA treatment and then monthly. The behavioral evaluation at the end of the study demonstrated a significant decrease in motor performance in mice treated with both doses of OTA as detected by the wire hang (control vs OTA 0.21 $p = 0.039$; control vs OTA 0.5 $p = 0.018$) (Fig. 1a) and the negative geotaxis tests (control vs OTA 0.21 $p = 0.048$; control vs OTA 0.5 $p = 0.024$) (Fig. 1b).

3.3. DA dysfunction induced by OTA treatment

Behavioral changes were associated with a loss of DA innervation reflected by a significant decrease in TH staining in the anterior (control

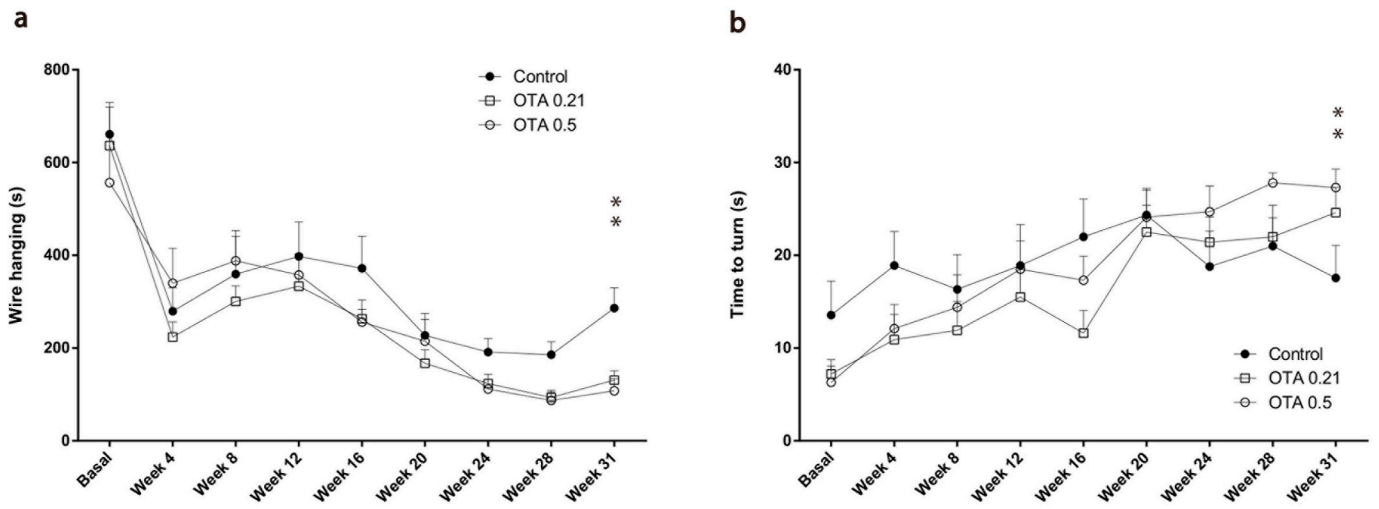

Fig. 1. Motor performance in mice exposed to oral subchronic doses of OTA. a) Wire hang performance of control and OTA treated Balb/c mice. b) Time to turn around and move up toward the top of the platform in the negative geotaxis test, if the mouse was unable to turn, the default value of 30 s was taken as maximal severity of impairment. Data are expressed as mean ± SEM (n = 9 control mice, n = 10 OTA-treated mice). Statistical significance was determined with two-way ANOVA test compared to control mice, *p < 0.05.

vs OTA 0.21: 18.6% decrease, $p = 0.011$; control vs OTA 0.5: 17.7% decrease, $p = 0.016$), medium (control vs OTA 0.21: 18.3% decrease, $p = 0.055$; control vs OTA 0.5: 26.8% decrease, $p = 0.005$) and posterior striatum (control vs OTA 0.21: 19.7% decrease, $p = 0.023$; control vs OTA 0.5: 31.8% decrease, $p = 0.000$) in both groups, a dose-response effect in the TH denervation was observed in all the striatum levels (Fig. 2a, Supp Fig 3). Although no volume alteration in the midbrain was observed, there was a significant 26% decrease in the number of TH+ DA neurons in the SNc in the group treated with 0.21 mg/kg OTA (Fig. 2b), although this was not significantly affected in the group treated with 0.5 mg/kg OTA (Fig. 2b) (control vs OTA 0.21 $p = 0.048$; control vs OTA 0.5 $p = 0.948$).

3.4. Changes in alpha-synuclein and chaperone-mediated autophagy protein levels related to OTA treatment

In order to investigate if the DA pathology was associated with changes in alpha-synuclein protein, we assessed the level of alpha-synuclein protein by Western blot in areas affected by alpha-synuclein pathology in different stages of PD (Braak staging). In the midbrain area (stage 3, clinical debut of PD) there was a significant 50% and a 10% (non-significant) increase respectively in the level of alpha-synuclein protein in mice treated with 0.21 and 0.5 mg/kg OTA (control vs OTA 0.21 $p = 0.027$; control vs OTA 0.5 $p = 1$) (Fig. 3a). The increase in total levels of alpha-synuclein in midbrain was associated with a 20% increase in the levels of S129 phosphorylated alpha-synuclein, although this increase did not reach statistical significance (control vs OTA 0.21 $p = 0.145$; control vs OTA 0.5 $p = 0.945$) (Fig. 3a), and the presence of phospho-alpha-synuclein aggregates in the SNc (Fig. 3b) (OTA 0.21: 1.5 aggregates per section, $p = 0.001$ vs control; OTA 0.5: 2.5 aggregates per section, $p = 0.000$ vs control). The level of alpha-synuclein protein in the brainstem (stage 2, pre-clinical PD) (control vs OTA 0.21 $p = 1$; control vs OTA 0.5 $p = 1$) and cortex (stages 4–6) (control vs OTA 0.21 $p = 1$; control vs OTA 0.5 $p = 1$) was not significantly increased in the groups treated with OTA (Supp Fig 4). Since the main pathway for alpha-synuclein degradation is CMA, we assessed the levels of 2 key proteins in the CMA pathway, LAMP-2A and hsc70, in midbrain. Our results demonstrated a dose-dependent decrease in LAMP-2A levels in the midbrain (OTA 0.21 20% decrease, $p = 0.251$; OTA 0.5 50% decrease, $p = 0.009$) (Fig. 3c). However, hsc70 protein levels were not significantly altered in midbrain at either OTA doses (Fig. 3c) (control vs OTA 0.21 $p = 0.347$; control vs OTA 0.5 $p = 0.056$).

3.5. Alpha-synuclein and CMA-related changes induced by OTA in intestinal tissue

In the gut there were increased levels of phosphorylated alpha-synuclein deposits in the myenteric, submucosal plexus and muscular layers (Fig. 4a), which covered significant larger area than in control mice (Fig. 4b) (control vs OTA 0.21 $p = 0.002$; control vs OTA 0.5 $p = 0.049$). There were also significantly increased total levels of alpha-synuclein protein in distal intestine (Fig. 4c) (control vs OTA 0.21 $p = 0.048$; control vs OTA 0.5 $p = 0.027$) and a dose-dependent decrease in LAMP-2A levels (0.21: 33% decrease, $p = 0.010$; 0.5: 32% decrease, $p = 0.018$) (Fig. 4d). hsc70 protein levels were unaltered in distal intestine (Fig. 4d) (control vs OTA 0.21 $p = 0.873$; control vs OTA 0.5 $p = 0.873$).

3.6. OTA induced CMA dysfunction in cell models

We established an intestinal epithelium (Caco-2) and neuronal (SH-SY5Y) over-expressing alpha-synuclein cell models to study the mechanism involved in the OTA induced alpha-synuclein and dopaminergic changes. Initially we assessed the range of subtoxic concentration of OTA (Fig. 5a and b) and a range of doses from 25 to 200 nM OTA were selected for the subsequent experiments. Doses between 80 and 200 nM increased significantly the intracellular alpha-synuclein levels in both cell models (Fig. 5c and d). In order to investigate the mechanism responsible for alpha-synuclein accumulation, we assessed alpha-synuclein turn-over as there is increasing evidence that alpha-synuclein degradation pathways may be compromised in PD (Alvarez-Erviti et al., 2010). Under control conditions alpha-synuclein half-life was 40.1 h; however, OTA treatment increased significantly alpha-synuclein half-life to 50.7 h (increased by 26%, $p = 0.043$) (Fig. 6a, Supp Fig 5). The decreased alpha-synuclein turn-over was related with a significant 45% decrease (control vs OTA 100 nM $p = 0.014$; control vs OTA 200 nM $p = 0.014$) in LAMP-2A protein levels (Fig. 6b), and a significant 48% decrease in lamp-2a mRNA levels with the 200 nM OTA (control vs OTA 100 nM $p = 0.487$; control vs OTA 200 nM $p = 0.00.37$) (Fig. 6c). None of the OTA concentrations significantly affected hsc70 protein (control vs OTA 100 nM $p = 0.219$; control vs OTA 200 nM $p = 0.219$) (Fig. 6b) or mRNA levels (control vs OTA 100 nM $p = 0.100$; control vs OTA 200 nM $p = 0.487$) (Fig. 6c).

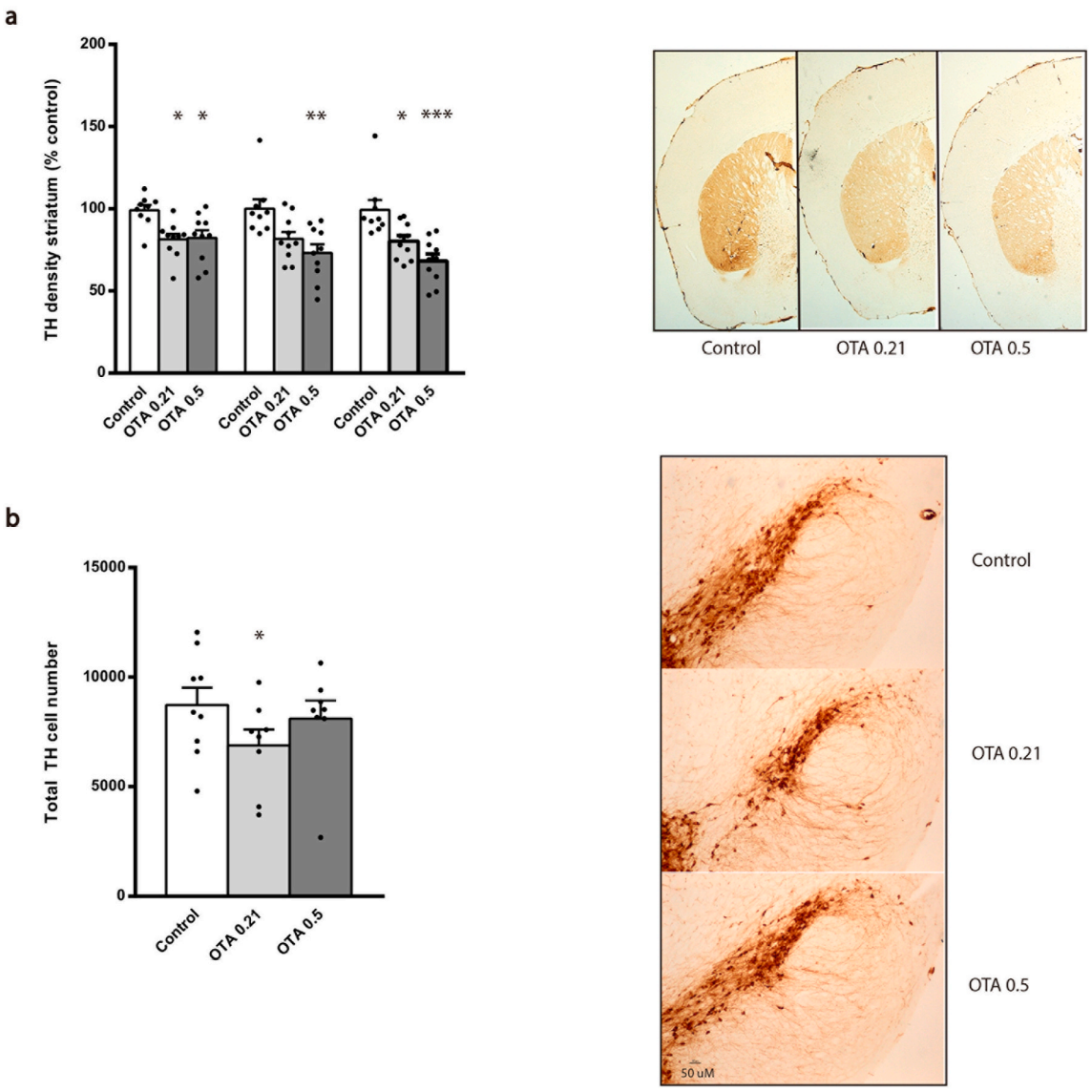

Fig. 2. Nigrostriatal dopaminergic dysfunction after 31 weeks in mice exposed to oral subchronic doses of OTA. a) Striatal TH innervation was quantified by optical density at 3 rostrocaudal levels (n = 9 for control mice; n = 9 for OTA 0.21 mg/kg; n = 10 for OTA 0.5 mg/kg). Images for TH staining in posterior striatum of control and OTA Balb/c mice are shown. b) Unbiased stereological quantification of TH-immunoreactive neurons in the SNc of Balb/c mice treated with 0.21 mg/kg (n = 8) and 0.5 mg/kg (n = 8) doses of OTA or Control (n = 9). Representative images of TH staining of dopaminergic neurons in coronal sections of the midbrain are shown. Scale bar represents 100 μm. Data are expressed as mean ± SEM, black dots correspond to individual animals, samples from animals not compiling with the quality criteria for the technique were not analyzed. One-way ANOVA test, statistical analyses compared to control mice, *p < 0.05, **p < 0.01, ***p < 0.001.

3.7. OTA influences on miRNA levels and the effects of hsa-miR-193a-3p up-regulation on LAMP-2A levels

As a previous report showed that miRNA dysregulation lead to the reported downregulation of LAMP-2A levels and compromised alpha-synuclein degradation (Alvarez-Erviti et al., 2013), the miRNA levels were analyzed in SH-SY5Y cells after exposure to OTA. Six miRNAs were significantly upregulated (hsa-miR-4792, hsa-miR-3196, hsa--miR-193a-3p, hsa-miR-6087, hsa-miR-24-2-5p, hsa-miR-513c-3p) and the level of 4 miRNAs (hsa-miR-1271–5p, hsa-miR-3607–5p, hsa-miR-99b-5p, hsa-miR-501–3p) were significantly downregulated (Fig. 6d, Supp Fig 6, 7). A miRNA target analysis using 5 target prediction tools (Diana/miRanda/miRBridge/PicTar/miRWalk) predicted hsa-miR-193a-3p to target *lamp-2a* mRNA. To determine the ability of hsa-miR-193a-3p to target the 3′UTR sequence of *lamp-2a*, we transfected SH-SY5Y cells with a luciferase reporter constructs with the *lamp-2a* 3′UTR sequence (Alvarez-Erviti et al., 2013). After 48h, 100 nM of hsa-miR-193a-3p caused a 39% decrease ($p = 0.00.37$) in luciferase activity linked to *lamp-2a* 3′UTR sequence (Fig. 6e).

3.8. Influence of changes in alpha-synuclein pathology on LAMP-2A

To determine if the changes in LAMP-2A levels could be secondary to the alpha-synuclein pathology, we analyzed the in vivo alpha-synuclein PFF mouse model. LAMP-2A and hsc70 protein levels in midbrain were evaluated at 3 time points, 15 dpi, 30 dpi and 90 dpi, which represent different stages of the alpha-synuclein pathology from the initial aggregation to the neuronal cell death. LAMP-2A protein levels were significantly decreased by 29%, 23% and 39% relative to actin at the 3 time points respectively (control vs 15 dpi $p = 0.012$; control vs 30 dpi $p = 0.012$; control vs 90 dpi $p = 0.012$) (Fig. 7a) but no significant changes in *lamp-2a* mRNA levels were observed (control vs 15 dpi $p = 0.347$; control vs 30 dpi $p = 0.823$; control vs 90 dpi $p = 1$) (Fig. 7b). The levels of hsc70 protein (control vs 15 dpi $p = 0.140$; control vs 30 dpi $p = 1$;

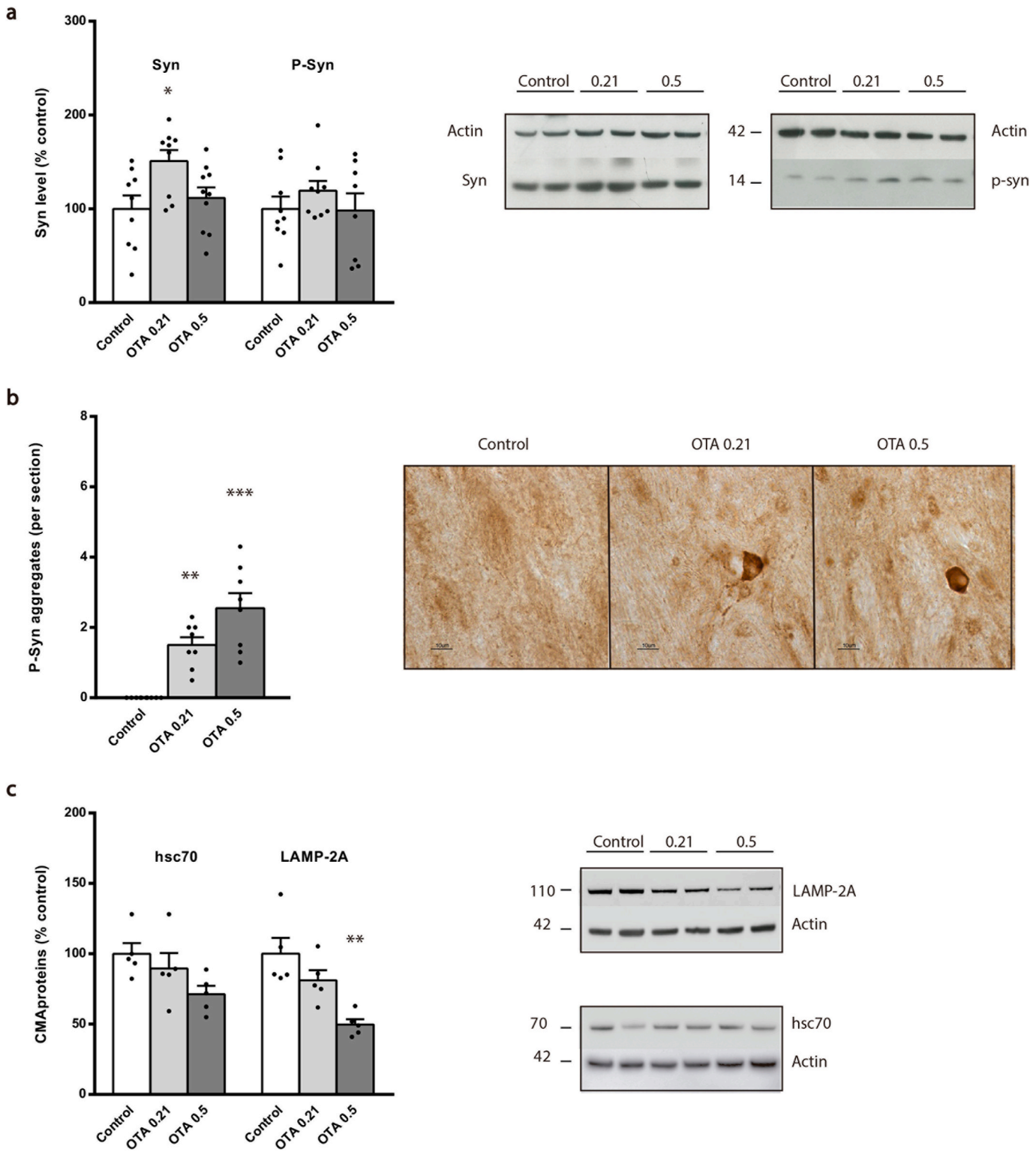

Fig. 3. Alpha-synuclein pathology in the midbrain at 31 weeks. a) Quantification of total (Syn) and phosphorylated alpha-synuclein (P-Syn) protein levels normalized to beta-actin in the midbrain (MB) of control and Balb/c mice orally treated with 0.21 mg/kg and 0.5 mg/kg doses of OTA (n = 9 for all groups). Typical Western blots are shown. b) Quantification of S129-phospho-alpha-synuclein positive aggregates in the SNc of control and OTA treated Balb/c mice. Representative images of intraneuronal phospho-alpha-synuclein inclusions in the SNc of mice orally treated with 0.21 mg/kg and 0.5 mg/kg doses of OTA are shown (n = 8 for all groups). Scale bars represent 10 μm. c) Protein levels of LAMP-2A and hsc70 normalized to beta-actin were quantified in the midbrain of Balb/c mice orally treated with 0.21 mg/kg and 0.5 mg/kg doses of OTA and controls (n = 5 for all groups). Data expressed as mean ± SEM, black dots correspond to individual animals. In some experiments, there was not enough tissue available from all the animals. One-way ANOVA test, statistical analyses compared with control mice, *$p < 0.05$, **$p < 0.05$, ***$p < 0.001$.

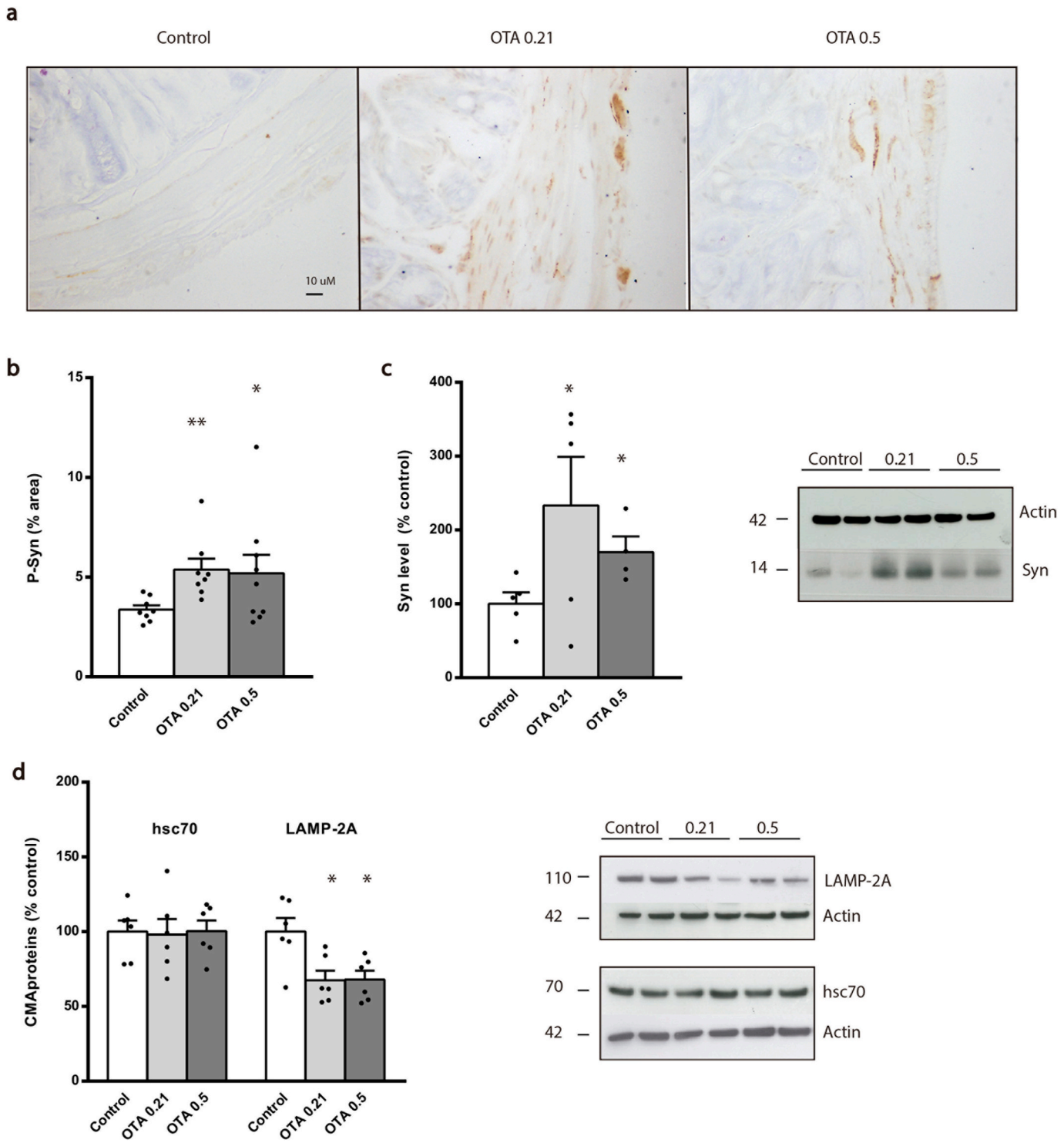

Fig. 4. Oral subchronic doses of OTA result in alpha-synuclein deposits in distal intestine at 31 weeks after OTA treatment. a) Representative images of distal intestine sections immunostained for S129-phospho-alpha-synuclein (P-Syn) in control and 0.21 mg/kg and 0.5 mg/kg OTA treated Balb/c mice 31 weeks after OTA treatment. Scale bar = 10 μm. b) Quantification of the percentage of area occupied by phosphorilated alpha-synuclein deposits in the distal intestine of control and OTA treated Balb/c mice (n = 8 for all groups). c) Analyses of alpha-synuclein protein levels normalized to beta-actin in the distal intestine (n = 5 for all groups). Typical Western blot is shown. d) Protein levels of LAMP-2A and hsc70 normalized to beta-actin were quantified in the distal intestine of Balb/c mice orally treated with 0.21 mg/kg and 0.5 mg/kg doses of OTA and controls (n = 5 for all groups). Data are expressed as mean ± SEM, black dots correspond to individual animals. One-way ANOVA test, statistical analyses compared with control mice, *p < 0.05.

control vs 90 dpi $p = 1$) (Fig. 7a) and mRNA (control vs 15 dpi $p = 1$; control vs 30 dpi $p = 1$; control vs 90 dpi $p = 1$) (Fig. 7b) were unaltered in midbrain at the 3 time points.

4. Discussion

The factors initiating or contributing to the pathogenesis of PD are a continuing source of controversy; many genetic factors have been

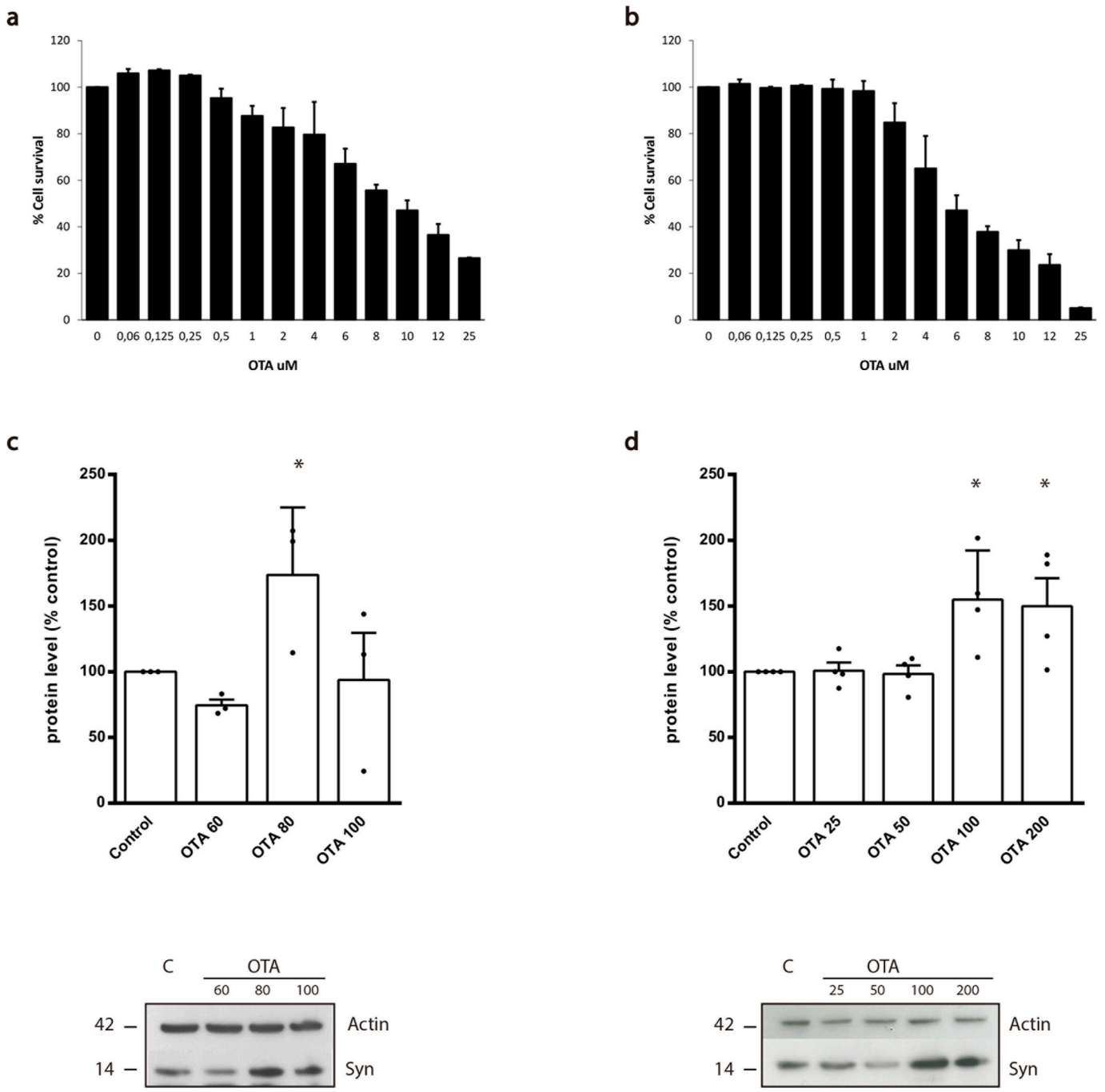

Fig. 5. Effect of OTA in cell models. Percentage of cell death in Caco-2 (a) and SH-SY5Y (b) cells treated with OTA (0.06–25 μM) 72 h (n = 3). Quantification of alpha-synuclein under control conditions and in the presence of OTA was determined in (c) Caco-2 (60–100 nM OTA, n = 3) and (d) SH-SY5Y (25–200 nM OTA, n = 4) cells by Western blot. Typical Western blot are shown. Data are expressed as mean ± SD. Non-parametric Kruskal-Wallis test, statistical analyses compared with untreated control group,*$p < 0.05$.

identified and environmental factors have long been suspected to be important and continue to be key factors associated with PD pathogenesis (Chen and Ritz, 2018; Pan-Montojo et al., 2012). Our study is the first to investigate the long term consequences of low dose of OTA exposure in the onset and progression of alpha-synuclein pathology and in the development of motor deficits in Balb/c WT mice. The exposure conditions selected (0.21 or 0.5 mg/kg bw by gavage for 4 weeks) are considered as very low doses for mice, as the lowest observed effect level for kidney tumors was 4.4 mg/kg bw (administered in diet) in 2 years bioassay (EFSA, 2006). Moreover, in our study no clinical signs of toxicity were observed at these doses either after the 28 days of exposure (preliminary study) in which OTA levels were detectable in plasma and brain, or during the 6 months in which animals were left under normal diet. Thus, observing any significant brain pathological changes in this study was not expected.

However, the results obtained in this study demonstrate that oral subchronic doses of OTA reproduce the key pathological features of PD, including motor deficits, decrease in the number of TH + DA neurons in the SNc and DA innervations in the striatum and the accumulation of phosphorylated alpha-synuclein within the CNS six months after the end of the OTA treatment. Two previous reports have investigated the neurotoxic effects of oral exposure to OTA in rodents. Belmadani et al.

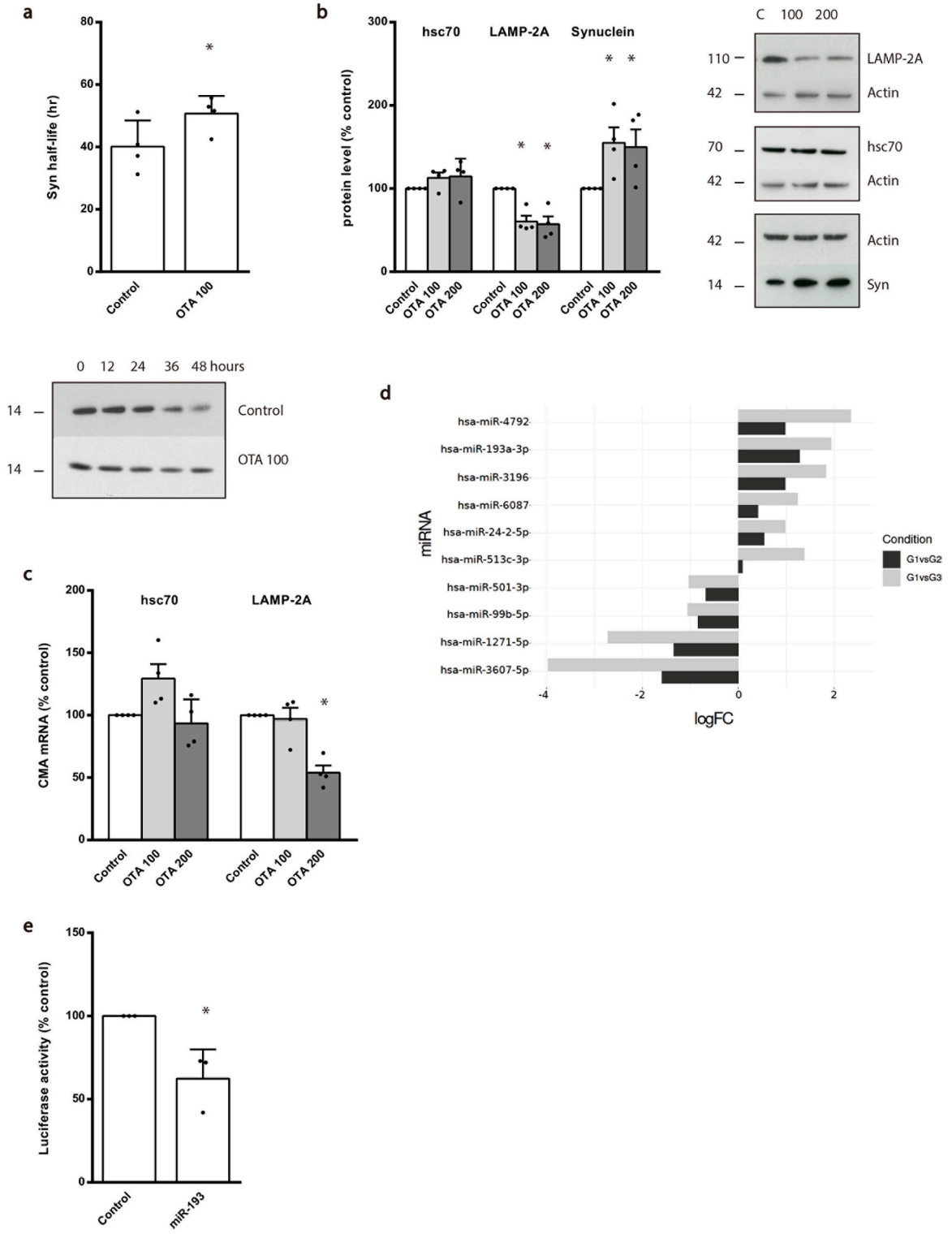

Fig. 6. Influence of OTA upon CMA and alpha-synuclein in cell cultures. a) Alpha-synuclein half-life was determined in SH-SY5Y cells by Western blot under control conditions and in the presence of OTA (100 nM). Typical Western blot are shown and OTA caused a significant decrease in alpha-synuclein turnover (n = 4). b) Steady state levels of alpha-synuclein, LAMP-2A and hsc70 relative to actin were detected by Western blot analyses in WT alpha-synuclein over-expressing cells 72 h after OTA treatment (100, 200 nM) and untreated cells (n = 4). Typical Western blot are shown and quantified relative to actin. c) *hsc70* and *lamp-2a* mRNA levels were quantified by qPCR in cells treated with OTA (100 nM) and controls and quantified relative to actin (n = 4). d) miRNA levels were quantified in cells treated with 100 nM OTA (group 2) or 200 nM OTA (group 3) relative to control cells (group 1) and data expressed as log FC change in miRNA levels e) Luciferase reporter assay in SHSY5Y cells expressing the 3′UTR of *lamp-2a Renilla* luciferase construct and incubated with 100 nM of has-miR-193a-3p or control (n = 3). *Renilla* luciferase activity is expressed normalized to untreated cells. Data expressed as mean ± SD, black dots correspond to independent experiments. Non-parametric Kruskal-Wallis test, statistical analyses compared with untreated control group, *$p < 0.05$.

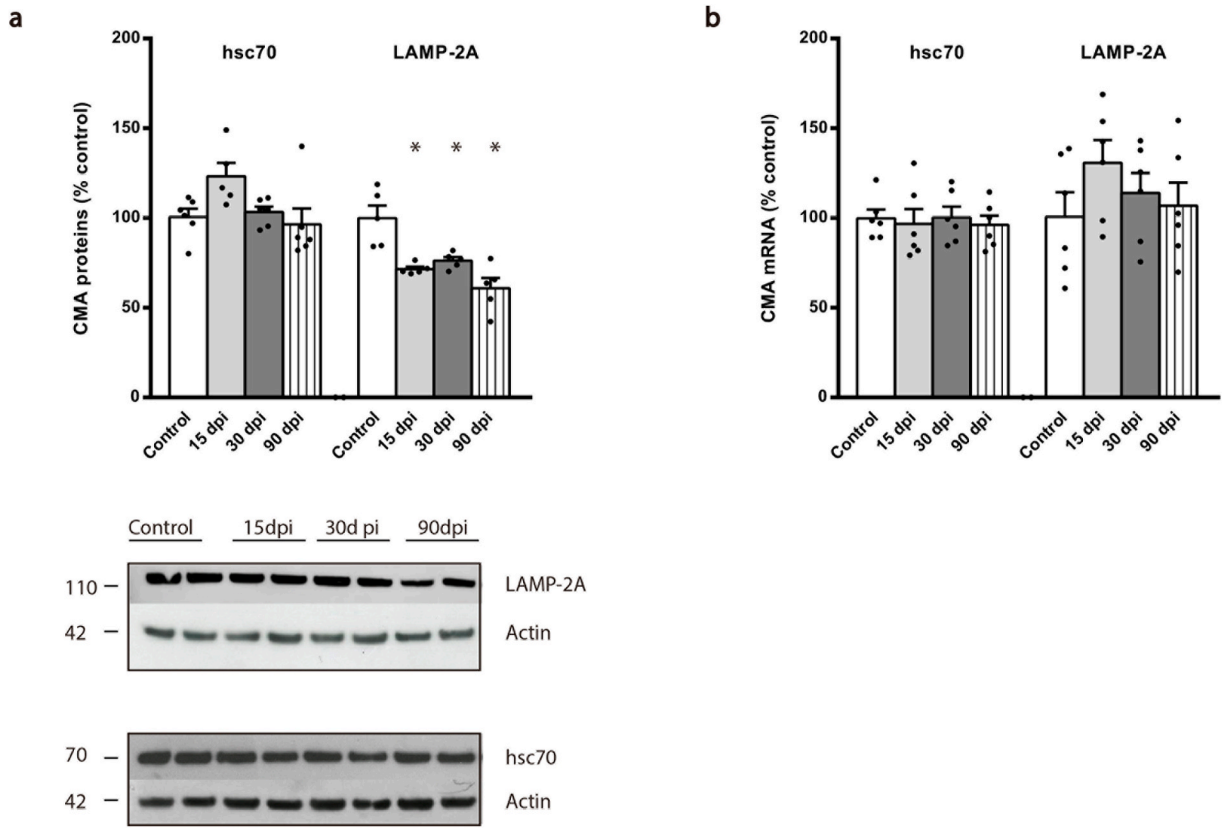

Fig. 7. CMA protein level in alpha-synuclein PFFs injected C57BL6/C3H F1 mice. (a) Quantification of LAMP-2A and hsc70 protein levels normalized to beta-actin in the midbrain in Control (PBS) and alpha-synuclein PFF injected C57BL6/C3H F1 mice 15, 30 and 90 dpi (n = 6). Typical Western blot are shown. b) *hsc70* and *lamp-2a* mRNA levels in Control (PBS) and alpha-synuclein PFF injected C57BL6/C3H F1 mice 15, 30 and 90 dpi (n = 6). Data expressed as mean ± SEM, black dots correspond to individual animals. One-way ANOVA test, statistical analyses compared with control mice, *p < 0.05, **p < 0.01.

(1998a,b) reported neurotoxic effects in striatum, hippocampus and ventral mesencephalon of adult male rats sub-chronically treated with OTA (289 μg/kg per 24h) by gastric intubation for 8 days (Belmadani et al., 1998a, b), and Sava et al. (2006) observed that continuous subcutaneous administration of low doses of OTA over a period of two weeks in mice causes significant depletion of striatal dopamine (Sava et al., 2006b). These authors argued that the neurotoxic effects of OTA could be a result of a direct effect of the toxin in the brain. However, our findings would suggest a different mechanism as the dopaminergic changes occurred after i) low doses of OTA administration for 28 days that reached systemic circulation and the brain and ii) months after the end of OTA treatment without detectable levels of OTA in plasma or brain.

In contrast to previous studies that used higher doses of OTA and evaluated the acute neurotoxic effects, we evaluated the pathological effects six months after the end of the low dose OTA treatment, when OTA levels were not anymore detectable in plasma and brain. The development of motor dysfunction months after the end of the treatment argues against a systemic or direct effect of OTA as causative factor but in turn points to a cascade of events that might be triggered by a sub-chronic exposure to OTA.

In this study we observed DA cell dysfunction related to increase in alpha-synuclein levels and presence of alpha-synuclein aggregation in the SNc. A dose-dependent reduction in the density of dopaminergic innervation was observed in the striatum, suggesting a DA cell dysfunction. In the SNc, this reduction in TH positive cells appeared to be significant only at the low dose, however in this case the variability between animals was also higher than in the case of the striatum. This effect might be related with the findings observed in a recent study that suggested that the impairment of terminals may precede the death of DA neurons (Matheoud et al., 2019). Thus, it could be possible that the time point selected for this study is relatively early regarding DA cell loss, and longer times after OTA treatment could be necessary to observe higher DA neuronal death in the SNc. In any case, the DA dysfunction is responsible for the motor impairments observed in the mice. All these alterations in DA system and motor function associated to alpha-synuclein pathology have been described previously in other animal model of PD based in the intrastriatal injection of alpha-synuclein PFF (Luck et al., 2012).

The Braak's hypothesis originally proposed that PD pathology may start in the ENS (or olfactory bulb) decades before spreading to the brain (Braak et al., 2006). Our results support this idea since an increase in alpha-synuclein levels was observed in the ENS and in anatomically connected brain regions, associated with the presence of some phospho-alpha-synuclein aggregates in the SNc. It should be noted that the slightly lower levels of alpha-synuclein expression detected in brain and intestine of samples from the 0.5 mg/kg OTA dose compared to the 0.21 mg/kg OTA dose could be related with the presence of higher levels of insoluble (aggregated) alpha-synuclein at the higher dose, that might difficult its extraction for the Western blot analysis. Nevertheless, further truncal vagotomy studies would be fundamental to confirm the spreading of alpha-synuclein from the gut to the brain through vagal nerve in mice orally exposed to low doses of OTA. Braak hypothesis is supported by the presence of alpha-synuclein pathology in the large intestine of PD patients years before diagnosis (Stockholm et al., 2016) and the fact that PD patients experience ENS dysfunction before the onset of motor symptoms (Cersosimo et al., 2013). In alpha-synuclein transgenic mice, alpha-synuclein aggregates have been detected in the ENS prior to any pathogenic changes in the CNS (Kuo et al., 2010) and intragastric administration of rotenone, a pesticide well known to

induce key pathological hallmarks of PD (Betarbet et al., 2000; Sherer et al., 2003), has also been demonstrated to induce alpha-synuclein accumulation in the ENS (Drolet et al., 2009; Pan-Montojo et al., 2010). We observed alpha-synuclein accumulation in the myenteric and submucosal plexus and muscular layer of the large intestine in mice orally exposed to low doses of OTA. Our results suggest that the changes in alpha-synuclein in the gut wall are a result of the OTA exposure and link with the changes to alpha-synuclein reported in the gut wall of PD patients (Stockholm et al., 2016). Indeed, OTA has been described able to disrupt the epithelial barrier (Robert et al., 2017). Although further studies are required to investigate the effects of OTA on gastrointestinal function and pathology, the results of our study indicate that exposure to low doses of OTA recapitulate the some pathological hallmark of PD in the ENS. However, it cannot be excluded that similar changes to those observed in intestine could be found in other organs, such us kidney.

Modeling the OTA treatment in cells we demonstrated that exposure to subtoxic OTA levels induces alpha-synuclein accumulation in Caco-2 and SH-SY5Y cells, the increase in alpha-synuclein observed was due to a decrease in the CMA protein LAMP-2A. Several publications reported LAMP-2A decrease in PD brains (Alvarez-Erviti et al., 2010; Murphy et al., 2015) and decrease LAMP-2A protein levels in cell culture resulted in significant alpha-synuclein intracellular accumulation (Alvarez-Erviti et al., 2010). We have previously proved that mitochondrial dysfunction, oxidative stress and increased alpha-synuclein levels did not decrease LAMP-2A protein levels (Alvarez-Erviti et al., 2013). However, several miRNAs increased in PD brains were experimentally shown to decrease LAMP-2A protein in cell models and resulted in significant alpha-synuclein accumulation (Alvarez-Erviti et al., 2013). OTA was related with miRNA dysfunction (Zhao et al., 2017) and we confirmed that exposure to subtoxic doses of OTA affected the expression of several miRNAs in SH-SY5Y cells. A miRNA significantly increased after OTA treatment, miRNA 193a-3p, was predicted to target the 3′UTR of *lamp-2a*. The luciferase reporter constructs confirmed that miRNA 193a-3p effectively targeted *lamp-2a* 3′UTRs, suggesting that could underpin the decrease in LAMP-2A reported in cells. As in the case of the in vivo study, the mechanistic hypothesis relevant for PD (alpha-synuclein, LAMP-2A and miRNA dysfunction) has been demonstrated at non-cytotoxic doses, pointing again to an early toxic endpoint that occurs before any cytotoxic damage to cells. These potential involvement of LAMP-2A protein in OTA pathological mechanisms was reinforced by the in vivo study, our results demonstrates that LAMP-2A protein expression was significantly reduced in the distal intestine and midbrain sites of alpha-synuclein pathology in OTA treated mice. Although we cannot exclude a direct effect of OTA upon LAMP-2A levels, the decrease in LAMP-2A protein in midbrain observed in the alpha-synuclein PFF model point to the abnormal pathological alpha-synuclein as the main cause of LAMP-2A decrease in OTA treated mice.

All these data pointed to a mechanism related to autophagy dysfunction common in mice exposed to low doses of OTA and PD patients and reinforce the hypothesis that links environmental factors exposure to mechanisms underlying the onset of PD.

These results are especially relevant in terms of human exposure, as humans are normally exposed to very low doses of OTA over their lifetime (EFSA, 2006 and 2020). On the other hand the current most sensitive effect considered for OTA risk assessment is its effects on kidneys in rats and pigs. In the most recent EFSA evaluation, in which a margin of exposure approach was used, the characterization of non-neoplastic effects was based on a $BMDL_{10}$ of 4.73 μg/kg bw per day calculated from kidney lesions observed in the pig study; while for neoplastic effects, a $BMDL_{10}$ of 14.5 μg/kg bw per day was calculated from kidney tumors seen in the rat study (EFSA, 2020). Thus taking into account that mice are less sensitive to OTA than rats (EFSA 2006 and 2020) and that in our experiment animals were only treated for 28 days, our results might be pointing to a more sensitive or early toxic endpoint than the one used for the current human health risk assessment of OTA.

Regarding neurotoxicity, in the first EFSA risk assessment (EFSA, 2006) this endpoint was also assessed based on effects reported at oral doses of 0.05–0.07 mg OTA/kg bw per day in rats (Wangikar et al., 2004; Dortant et al., 2001) and rabbits (Wangikar et al., 2005) and with 3 mg OTA/kg bw per day in mice (Sava et al., 2006a). The conclusion (EFSA, 2006) was that the lowest neurotoxic dose of OTA (50 μg/kg) was about six times higher than the dose leading to minimal renal changes observed in the pivotal studies for nephrotoxicity (EFSA, 2006). However, it should be mentioned that the studies available were not designed to evaluate neurodegenerative endpoints. In the most recent evaluation, EFSA (2020) also pointed to the nervous system as another potential toxicological endpoint, together with the immune, the intestinal and endocrine systems.

5. Conclusions

In conclusion, we demonstrated that oral exposure to low doses of OTA causes alterations in motor function, DA system and alpha-synuclein pathology several months after the end of the treatment. We propose that the initiation of this Parkinson-like pathology is due to a decrease in LAMP-2A protein levels in the gut caused by the OTA induced miRNA dysregulation and propagation of the alpha-synuclein pathology involves a prion-like mechanism. All these features have been previously related and described in PD. This supports the hypothesis that environmental factors could play a key role in PD, adding a further dimension to the pathogenesis of PD and LB formation.

Ethics approval and consent to participate

All applicable international, national, and/or institutional guidelines for the care and use of animals were followed. All procedures performed in studies involving animals were in accordance with the ethical standards of the institution or practice at which the studies were conducted (name of committee: Órgano Encargado del Bienestar Animal del Centro de Investigación Biomédica de La Rioja, OEBA-CIBIR; permit number: LAE-02, LAE-04).

Consent for publication

Not applicable.

Availability of data and materials

All primary data and materials will be made available under request.

Funding

This study was funded by European Regional Development Fund (ERDF) “A way to make Europe” (6FRSABC008), the Government of Navarra (Project-43, 2019 modality A) and European Regional Development Fund (ERDF under Operational Programme for Navarra, 2014–2020). Chromatographic studies were funded by the “Ministerio de Economia, Industria y Competitividad, Agencia Estatal de Investigacion” (AGL2017-85732-R) (MINECO/AEI/FEDER, UE). L.A.E is supported by a Miguel Servet contract (CP15/00200) from ISCIII. F.J.B is supported by a Miguel Servet contract (CP19/00200) from ISCIII.

Author contributions

M.I, A.V, A.L.C, J.M.C and L.A.E. contributed to the study conception, design and discussion of the results. M.I. and R.F performed and analyzed the mouse experiments. L.A.E. and N.A.H performed and analyzed cell experiments. F.J.B. performed stereological analysis. M.D. T. performed primary and differential analysis of the miRNA-seq data. A. V. and E.G.P. performed the chromatographic quantification of OTA in brain and plasma samples. All authors read and approved the final manuscript.

Declaration of competing interest

The authors declare that they have no known competing financial interests or personal relationships that could have appeared to influence the work reported in this paper.

Acknowledgments

Not applicable.

List of abbreviations

bw	body weight
CMA	Chaperone mediated-autophagy
CNS	Central Nervous System
DA	dopaminergic
dpi	days post injection
ENS	Enteric Nervous System
LB	Lewy body
MoA	mode of action
MPTP	1-methyl-4-phenyl-1,2,3,6-tetrahydropyridine
OD	optical density
OTA	Ochratoxin A
PD	Parkinson's disease
PFF	preformed fibrils
SNc	substantia nigra pars compacta
TH	tyrosine hydroxylase
WT	wild type

Appendix A. Supplementary data

Supplementary data to this article can be found online at https://doi.org/10.1016/j.fct.2021.112164.

References

Adaku Chilaka, C., Mally, A., 2020. Mycotoxin occurrence, exposure and health implications in infants and young children in sub-saharan Africa: a Review. Foods 9, 1585. https://doi.org/10.3390/foods9111585. PMID: 33139646.

Alvarez-Erviti, L., Rodriguez-Oroz, M.C., Cooper, J.M., Caballero, C., Ferrer, I., Obeso, J. A., Schapira, A.H., 2010. Chaperone-mediated autophagy markers in Parkinson disease brains. Arch. Neurol. 67, 1464–1472. https://doi.org/10.1001/archneurol.2010.198. PMID: 20697033.

Alvarez-Erviti, L., Seow, Y., Schapira, A.H., Rodriguez-Oroz, M.C., Obeso, J.A., Cooper, J. M., 2013. Influence of microRNA deregulation on chaperone-mediated autophagy and α-synuclein pathology in Parkinson's disease. Cell Death Dis. 4, e545. https://doi.org/10.1038/cddis.2013.73. PMID: 23492776.

Andrés-León, E., Núñez-Torres, R., Rojas, A.M., 2016. miARma-Seq: a comprehensive tool for miRNA, mRNA and circRNA analysis. Sci. Rep. 6, 25749. https://doi.org/10.1038/srep25749. PMID: 27167008.

Anselmi, L., Bove, C., Coleman, F.H., Le, K., Subramanian, M.P., Venkiteswaran, K., Subramanian, T., Travagli, R.A., 2018. Ingestion of subthreshold doses of environmental toxins induces ascending parkinsonism in the rat. NPJ Parkinsons Dis 4, 30. https://doi.org/10.1038/s41531-018-0066-0. PMID: 30302391.

Arce-López, B., Lizarraga, E., Vettorazzi, A., González-Peñas, E., 2020. Human biomonitoring of mycotoxins in blood, plasma and serum in recent years: a review. Toxins 12, 147. https://doi.org/10.3390/toxins12030147. PMID: 32121036.

Belmadani, A., Tramu, G., Betbeder, A.M., Steyn, P.S., Creppy, E.E., 1998a. Regional selectivity to ochratoxin A, distribution and cytotoxicity in rat brain. Arch. Toxicol. 72, 656–662. https://doi.org/10.1007/s002040050557. PMID: 9851682.

Belmadani, A., Tramu, G., Betbeder, A.M., Creppy, E.E., 1998b. Subchronic effects of ochratoxin A on young adult rat brain and partial prevention by aspartame, a sweetener. Hum. Exp. Toxicol. 17, 380–386. https://doi.org/10.1177/096032719801700704. PMID: 9726534.

Betarbet, R., Sherer, T.B., MacKenzie, G., Garcia-Osuna, M., Panov, A.V., Greenamyre, J. T., 2000. Chronic systemic pesticide exposure reproduces features of Parkinson's disease. Nat. Neurosci. 3, 1301–1306. https://doi.org/10.1038/81834. PMID: 11100151.

Bhat, P.V., Anand, T., Mohan Manu, T., Khanum, F., 2018. Restorative effect of l-Dopa treatment against Ochratoxin A induced neurotoxicity. Neurochem. Int. 118, 252–263. https://doi.org/10.1016/j.neuint.2018.04.003. PMID: 29627381.

BIOMIN, 2018. World Mycotoxin Survey. Annual Report 2018.

Braak, H., Del Tredici, K., Rüb, U., de Vos, R.A., Jansen Steur, E.N., Braak, E., 2003. Staging of brain pathology related to sporadic Parkinson's disease. Neurobiol. Aging 24, 197–211. https://doi.org/10.1016/s0197-4580(02)00065-9. PMID: 12498954.

Braak, H., Bohl, J.R., Müller, C.M., Rüb, U., de Vos, R.A., Del Tredici, K., 2006. Stanley Fahn Lecture 2005: the staging procedure for the inclusion body pathology associated with sporadic Parkinson's disease reconsidered. Mov. Disord. 21, 2042–2051. https://doi.org/10.1002/mds.21065. PMID: 17078043.

Brichta, L., Shin, W., Jackson-Lewis, V., Blesa, J., Yap, E.L., Walker, Z., et al., 2015. Identification of neurodegenerative factors using translatome-regulatory network analysis. Nat. Neurosci. 18, 1325–1333. https://doi.org/10.1038/nn.4070. PMID: 26214373.

Brooks, A.I., Chadwick, C.A., Gelbard, H.A., Cory-Slechta, D.A., Federoff, H.J., 1999. Paraquat elicited neurobehavioral syndrome caused by dopaminergic neuron loss. Brain Res. 823, 1–10. https://doi.org/10.1016/s0006-8993(98)01192-5. PMID: 10095006.

Cersosimo, M.G., Raina, G.B., Pecci, C., Pellene, A., Calandra, C.R., Gutiérrez, C., et al., 2013. Gastrointestinal manifestations in Parkinson's disease: prevalence and occurrence before motor symptoms. J. Neurol. 260, 1332–1338. https://doi.org/10.1007/s00415-012-6801-2. PMID: 23263478.

Chen, H., Ritz, B., 2018. The search for environmental causes of Parkinson's disease: moving forward. J Parkinson Dis 8, S9–S17. https://doi.org/10.3233/JPD-181493. PMID: 30584168.

Comi, C., Magistrelli, L., Oggioni, G.D., Carecchio, M., Fleetwood, T., Cantello, R., Mancini, F., Antonini, A., 2014. Peripheral nervous system involvement in Parkinson's disease: evidence and controversies. Park. Relat. Disord. 20, 1329–1334. https://doi.org/10.1016/j.parkreldis.2014.10.010. PMID: 25457816.

Costa, J., Ahluwalia, A., 2019. Advances and current challenges in intestinal in vitro model engineering: a digest. Front Bioeng Biotechnol 7, 144. https://doi.org/10.3389/fbioe.2019.00144. PMID: 31275931.

Dellafiora, L., Dall'Asta, C., 2017. Forthcoming challenges in mycotoxins toxicology research for safer food—a need for Multi-Omics approach. Toxins 9, 18. https://doi.org/10.3390/toxins9010018. PMCID: PMC5308250.

Dortant, P.M., Peters-Volleberg, G.W.M., VanLoveren, H., Marquardt, R.R., Speijers, G.J. A., 2001. Age-related differences in the toxicity of ochratoxin A in female rats. Food Chem. Toxicol. 39 (1), 55–65. https://doi.org/10.1016/s0278-6915(00)00107-1. PMID: 11259851.

Drolet, R.E., Cannon, J.R., Montero, L., Greenamyre, J.T., 2009. Chronic rotenone exposure reproduces Parkinson's disease gastrointestinal neuropathology. Neurobiol. Dis. 36, 96–102. https://doi.org/10.1016/j.nbd.2009.06.017. PMID: 19595768.

No 1881/2006 of 19 December Commission Regulation (EC), 2006. Setting Maximum Levels for Certain Contaminants in Foodstuffs (Text with EEA Relevance). Consolidated version 28/11/2019.

EFSA (European Food Safety Authority), 2006. Opinion of the scientific panel on contaminants in the food chain on a request from the commission related to ochratoxin A in food. EFSA Journal 4 (6), 1–56. https://doi.org/10.2903/j.efsa.2006.365, 365.

EFSA CONTAM Panel (EFSA Panel on Contaminants in the Food Chain), 2020. Scientific Opinion on the risk assessment of ochratoxin A in food. EFSA Journal 2020 18 (5), 150. https://doi.org/10.2903/j.efsa.2020.6113, 6113.

Eskola, M., Kos, G., Elliott, C.T., Hajšlová, J., Mayar, S., Krska, R., 2019. Worldwide contamination of food-crops with mycotoxins: validity of the widely cited 'FAO estimate' of 25. Crit. Rev. Food Sci. Nutr. 3, 1–17. https://doi.org/10.1080/10408398.2019.1658570. PMID: 31478403.

Fearnley, J.M., Lees, A.J., 1991. Ageing and Parkinson's disease: substantia nigra regional selectivity. Brain 114, 2283. https://doi.org/10.1093/brain/114.5.2283. PMID: 1933245.

Goldman, S.M., 2014. Environmental toxins and Parkinson's disease. Annu. Rev. Pharmacol. Toxicol. 54, 141–164. https://doi.org/10.1146/annurev-pharmtox-011613-135937. PMID: 24050700.

Gorell, J.M., Johnson, C.C., Rybicki, B.A., Peterson, E.L., Richardson, R.J., 1998. The risk of Parkinson's disease with exposure to pesticides, farming, well water, and rural living. Neurology 50, 1346–1350. https://doi.org/10.1212/wnl.50.5.1346. PMID: 95959851.

Hatcher, J.M., Pennell, K.D., Miller, G.W., 2008. Parkinson's disease and pesticides: a toxicological perspective. Trends Pharmacol. Sci. 29, 322–329. https://doi.org/10.1016/j.tips.2008.03.007. PMID: 18453001.

Hawkes, H., Del Tredici, K., Braak, H., 2007. Parkinson's disease: a dual-hit hypothesis. Neuropathol. Appl. Neurobiol. 33, 599–614. https://doi.org/10.1111/j.1365-2990.2007.00874.x. PMID: 17961138.

Hong, J.T., Lee, M.K., Park, K.S., Jung, K.M., Lee, R.D., Jung, H.K., et al., 2002. Inhibitory effect of peroxisome proliferator-activated receptor gamma agonist on ochratoxin A-induced cytotoxicity and activation of transcription factors in cultured rat embryonic midbrain cells. J. Toxicol. Environ. Health 65, 407–418. https://doi.org/10.1080/15287390252808073. PMID: 11936221.

IARC, 1993. Some naturally occurring substances: food items and constituents, heterocyclic aromatic amines and mycotoxins. IARC Monogr. Eval. Carcinog. Risks Hum. 56, 489–521.

Ito, T., Uchida, K., Nakayama, H., 2013. Neuronal or inducible nitric oxide synthase (NOS) expression level is not involved in the different susceptibility to nigro-striatal dopaminergic neurotoxicity induced by 1-methyl-4-phenyl-1,2,3,6-tetrahydropyridine (MPTP) between C57BL/6 and BALB/c mice. Exp. Toxicol. Pathol. 65, 121–125. https://doi.org/10.1016/j.etp.2011.06.009.

Janik, E., Niemcewicz, M., Ceremuga, M., Stela, M., Saluk-Bijak, J., Siadkowski, A., Bijak, M., 2020. Molecular aspects of mycotoxins-A serious problem for human health. Int. J. Mol. Sci. 21, E8187. https://doi.org/10.3390/ijms21218187. PMID: 33142955.

Johnson, M., Stecher, B., Labrie, V., Brundin, L., Brundin, P., 2018a. Triggers, facilitators, and aggravators: redefining Parkinson's disease pathogenesis. Trends Neurosci. 42, 4–13. https://doi.org/10.1016/j.tins.2018.09.007. PMID: 30342839.

Johnson, M.E., Stringer, A., Bobrovskaya, L., 2018b. Rotenone induces gastrointestinal pathology and microbiota alterations in a rat model of Parkinson's disease. Neurotoxicology 65, 174–185. https://doi.org/10.1016/j.neuro.2018.02.013. PMID: 29471018.

Kett, L.R., Stiller, B., Bernath, M.M., Tasset, I., Blesa, J., Jackson-Lewism, V., et al., 2015. α-Synuclein-independent histopathological and motor deficits in mice lacking the endolysosomal Parkinsonism protein Atp13a2. J. Neurosci. 35, 5724–5742. https://doi.org/10.1523/JNEUROSCI.0632-14.2015. PMID: 25855184.

Khezri, A., Herranz-Jusdado, J.G., Ropstad, E., Fraser, T.W., 2018. Mycotoxins induce developmental toxicity and behavioural aberrations in zebrafish larvae. Environ. Pollut. 242, 500–506. https://doi.org/10.1016/j.envpol.2018.07.010. PMID: 30005262.

Kim, S., Kwon, S.H., Kam, T.I., Panicker, N., Karuppagounder, S.S., Lee, S., et al., 2019. Transneuronal propagation of pathologic α-synuclein from the gut to the brain models Parkinson's disease. Neuron 103, 627–641. https://doi.org/10.1016/j.neuron.2019.05.035. PMID: 31255487.

Kuo, Y.M., Li, Z., Jiao, Y., Gaborit, N., Pani, A.K., Orrison, B.M., et al., 2010. Extensive enteric nervous system abnormalities in mice transgenic for artificial chromosomes containing Parkinson disease-associated alpha-synuclein gene mutations precede central nervous system changes. Hum. Mol. Genet. 19, 1633–1650. https://doi.org/10.1093/hmg/ddq038. PMID: 20106867.

Langston, J.W., Ballard Jr., P.A., 1983. Parkinson's disease in a chemist working with 1-methyl-4-phenyl-1,2,5,6-tetrahydropyridine. N. Engl. J. Med. 309, 310. https://doi.org/10.1056/nejm198308043090511. PMID: 6602944.

Lock, E.A., Hard, G.C., 2004. Chemically induced renal tubule tumors in the laboratory rat and mouse: review of the NCI/NTP database and categorization of renal carcinogens based on mechanistic information. Crit. Rev. Toxicol. 34, 211–299. https://doi.org/10.1080/10408440490265210. PMID: 15239388.

Luk, K.C., Kehm, V., Carroll, J., Zhang, B., O'Brien, P., Trojanowski, J.Q., Lee, V.M., 2012. Pathological α-synuclein transmission initiates Parkinson-like neurodegeneration in nontransgenic mice. Science 338, 949–953. https://doi.org/10.1126/science.1227157. PMID: 23161999.

Marin, S., Ramos, A.J., Cano-Sancho, G., Sanchis, V., 2013. Mycotoxins: occurrence, toxicology, and exposure assessment. Food Chem. Toxicol. 60, 218–237. https://doi.org/10.1016/j.fct.2013.07.047. PMID: 23907020.

Marras, C., Canning, C.G., Goldman, S.M., 2019. Environment, lifestyle, and Parkinson's disease: implications for prevention in the next decade. Mov. Disord. 34, 801–811. https://doi.org/10.1002/mds.27720. PMID: 31091353.

Matheoud, D., Cannon, T., Voisin, A., Penttinen, A.M., Ramet, L., Fahmy, A.M., et al., 2019. Intestinal infection triggers Parkinson's disease-like symptoms in Pink1-/- mice. Nature 571, 565–569. https://doi.org/10.1038/s41586-019-1405-y. PMID: 31316206.

Murphy, K.E., Gysbers, A.M., Abbott, S.K., Spiro, A.S., Furuta, A., Cooper, A., et al., 2015. Lysosomal-associated membrane protein 2 isoforms are differentially affected in early Parkinson's disease. Mov. Disord. 30, 1639–1644. https://doi.org/10.1002/mds.26141. PMID: 25594542.

Niculita-Hirzel, H., Hantier, G., Storti, F., Plateel, G., Roger, T., 2016. Frequent occupational exposure to Fusarium Mycotoxins of workers in the Swiss grain industry. Toxins 8, 370. https://doi.org/10.3390/toxins8120370. PMID: 27973454.

National Toxicology Program (NTP), 2016. Report on Carcinogens, fourteenth ed.

Pan-Montojo, F., Anichtchik, O., Dening, Y., Knels, L., Pursche, S., Jung, R., et al., 2010. Progression of Parkinson's disease pathology is reproduced by intragastric administration of rotenone in mice. PloS One 5, e8762. https://doi.org/10.1371/journal.pone.0008762. PMID: 20098733.

Pan-Montojo, F., Schwarz, M., Winkler, C., Arnhold, M., O'Sullivan, G.A., Pal, A., et al., 2012. Environmental toxins trigger PD-like progression via increased alpha-synuclein release from enteric neurons in mice. Sci. Rep. 2, 898. https://doi.org/10.1038/srep00898. PMID: 23205266.

Park, S., Lim, W., You, S., Song, G., 2019. Ochratoxin A exerts neurotoxicity in human astrocytes through mitochondria-dependent apoptosis and intracellular calcium overload. Toxicol. Lett. 313, 42–49. https://doi.org/10.1016/j.toxlet.2019.05.021. PMID: 31154016.

Priyadarsh, i A., Khuder, S.A., Schaub, E.A., Priyadarshi, S.S., 2001. Environmental risk factors and Parkinson's disease: a metaanalysis. Environ. Res. 86, 122–127. https://doi.org/10.1006/enrs.2001.4264. PMID: 11437458.

Quandt, S.A., Walker, F.O., Talton, J.W., Summers, P., Chen, H., McLeod, D.K., Arcury, T. A., 2016. Olfactory function in Latino farmworkers: subclinical neurological effects of pesticide exposure in a vulnerable population. J. Occup. Environ. Med. 58, 248–253. https://doi.org/10.1097/JOM.0000000000000672. PMID: 26949874.

RASFF, 2019. The Rapid Alert System for Food and Feed — Annual Report.

Robert, H., Payros, D., Pinton, P., Théodorou, V., Mercier-Bonin, M., Oswald, I.P., 2017. Impact of mycotoxins on the intestine: are mucus and microbiota new targets? J. Toxicol. Environ. Health B Crit. Rev. 20, 249–275. https://doi.org/10.1080/10937404.2017.1326071. PMID: 28636450.

Sasajima, H., Miyazono, S., Noguchi, T., Kashiwayanagi, M., 2015. Intranasal administration of rotenone in mice attenuated olfactory functions through the lesion of dopaminergic neurons in the olfactory bulb. Neurotoxicology 51, 106–115. https://doi.org/10.1016/j.neuro.2015.10.006. PMID: 26493152.

Sava, V., Reunova, O., Velasquez, A., Harbison, R., Sánchez-Ramos, J., 2006a. Acute neurotoxic effects of the fungal metabolite ochratoxin-A. Neurotoxicology 27, 82–92. https://doi.org/10.1016/j.neuro.2005.07.004. PMID: 16140385.

Sava, V., Reunova, O., Velasquez, A., Sanchez-Ramos, J., 2006b. Can low level exposure to ochratoxin-A cause parkinsonism? J. Neurol. Sci. 249, 68–75. https://doi.org/10.1016/j.jns.2006.06.006. PMID: 16844142.

Schapira, A.H.V., Chaudhuri, K.R., Jenner, P., 2017. Non-motor features of Parkinson disease. Nat. Rev. Neurosci. 18, 435–450. https://doi.org/10.1038/nrn.2017.91. PMID: 28720825.

Sherer, T.B., Kim, J.H., Betarbet, R., Greenamyre, J.T., 2003. Subcutaneous rotenone exposure causes highly selective dopaminergic degeneration and alpha-synuclein aggregation. Exp. Neurol. 179, 9–16. https://doi.org/10.1006/exnr.2002.8072. PMID: 12504863.

Simón-Sánchez, J., Schulte, C., Bras, J.M., Sharma, M., Gibbs, J.R., Berg, D., et al., 2009. Genome-wide association study reveals genetic risk underlying Parkinson's disease. Nat. Genet. 41, 1308–1312. https://doi.org/10.1038/ng.487. PMID: 19915575.

Stirpe, P., Hoffman, M., Badiali, D., Colosimo, C., 2016. Constipation: an emerging risk factor for Parkinson's disease? Eur. J. Neurol. 23, 1606–1613. https://doi.org/10.1111/ene.13082. PMID: 27444575.

Stockholm, M.G., Danielsen, E.H., Hamilton-Dutoit, S.J., Borghammer, P., 2016. Pathological α-synuclein in gastrointestinal tissues from prodromal Parkinson disease patients. Ann. Neurol. 79, 940–949. https://doi.org/10.1002/ana.24648. PMID: 27015771.

Stoev, S.D., 2020. Long term preliminary studies on toxic and carcinogenic effect of individual or simultaneous exposure to ochratoxin A and penicillic acid in mice. Toxicon 184, 192–201. https://doi.org/10.1016/j.toxicon.2020.06.013. PMID: 32569847.

Susick, L.L., Lowing, J.L., Bosse, K.E., Hildebrandt, C.C., Chrumka, A.C., Conti, A.C., 2014. Adenylyl cylases 1 and 8 mediate select striatal-dependent behaviors and sensitivity to ethanol stimulation in the adolescent period following acute neonatal ethanol exposure. Behav. Brain Res. 269, 66–74. https://doi.org/10.1016/j.bbr.2014.04.031. PMID: 24769171.

Svensson, E., Horváth-Puhó, E., Thomsen, R.W., Djurhuus, J.C., Pedersen, L., Borghammer, P., et al., 2015. Vagotomy and subsequent risk of Parkinson's disease. Ann. Neurol. 78, 522–529. https://doi.org/10.1002/ana.24448. PMID: 26031848.

Thuvander, A., Breitholtz-Emanuelsson, A., Olsen, M., 1995. Effects of ochratoxin A on the mouse immune system after subchronic exposure. Food Chem. Toxicol. 33, 1005–1011. https://doi.org/10.1016/0278-6915(95)00075-5. PMID: 8846995.

Van der Mark, M., Brouwer, M., Kromhout, H., Nijssen, P., Huss, A., Vermeulen, R., 2012. Is pesticide use related to Parkinson disease? Some clues to heterogeneity in study results. Environ. Health Perspect. 120, 340–347. https://doi.org/10.1289/ehp.1103881. PMID: 22389202.

Vettorazzi, A., López de Cerain, A., 2016. Mycotoxins as food carcinogens. In: Viegas, C., et al. (Eds.), Environmental Mycology in Public Health. Academic Press- Elsevier, USA, pp. 261–298.

Vettorazzi, A., Gonzalez-Penas, E., Arbillaga, L., Corcuera, L.A., Lopez de Cerain, A., 2008. Simple high-performance liquid chromatography-fluorescence detection method for plasma, kidney and liver of rat as a tool for toxicology studies. J. Chromatogr. 1215, 100–106. https://doi.org/10.1016/j.chroma.2008.10.119. PMID: 19027908.

Viegas, S., Assunção, R., Nunes, C., Osteresch, B., Twarużek, M., Kosicki, R., et al., 2018. Exposure assessment to mycotoxins in a Portuguese fresh bread dough Company by using a multi-biomarker approach. Toxins 10, 342. https://doi.org/10.3390/toxins10090342. PMID: 30142887.

Wangikar, P.B., Dwivedi, P., Sharma, A.K., Sinha, N., 2004. Effect in rats of simultaneous prenatal exposure to ochratoxin A and aflatoxin B1. II. Histopathological features of teratological anomalies induced in fetuses. Birth Defects Res B Dev Reprod Toxicol 71, 352–358. https://doi.org/10.1002/bdrb.20022. PMID: 15617025.

Wangikar, P.B., Dwivedi, P., Sinha, N., Sharma, A.K., Telang, A.G., 2005. Teratogenic effects in rabbits of simultaneous exposure to ochratoxin A and aflatoxin B1 with special reference to microscopic effects. Toxicology 215, 37–47. https://doi.org/10.1016/j.tox.2005.06.022. PMID: 16054743.

West, 1993. M.J. New stereological methods for counting neurons. Neurobiol. Aging 14, 275–285. https://doi.org/10.1016/0197-4580(93)90112-o. PMID: 8367009.

WHO (World Health Organization), 2008. Safety evaluation of certain food additives and contaminants. WHO Food Addit. Ser. No. 59, 357–429.

Zhang, J., Fitsanakis, V.A., Gu, G., Jing, D., Ao, M., Amarnath, V., Montine, T.J., 2003. Manganese ethylene-bis-dithiocarbamate and selective dopaminergic neurodegeneration in rat: a link through mitochondrial dysfunction. J. Neurochem. 84, 336–346. https://doi.org/10.1046/j.1471-4159.2003.01525.x. PMID: 12558996.

Zhao, J., Qi, X., Dai, Q., He, X., Dweep, H., Guo, M., et al., 2017. Toxicity study of ochratoxin A using HEK293 and HepG2 cell lines based on microRNA profiling. Hum. Exp. Toxicol. 36, 8–22. https://doi.org/10.1177/0960327116632048. PMID: 26893291.

Zurich, M.G., Lengacher, S., Braissant, O., Monnet-Tschudi, F., Pellerin, L., Honegger, P., 2005. Unusual astrocyte reactivity caused by the food mycotoxin ochratoxin A in aggregating rat brain cell cultures. Neuroscience 134, 771–782. https://doi.org/10.1016/j.neuroscience.2005.04.030. PMID: 15994020.